Canada Alberta

**FOREST RESOURCE DEVELOPMENT AGREEMENT**
**ENTENTE SUR LA MISE EN VALEUR DES RESSOURCES FORESTIERES**

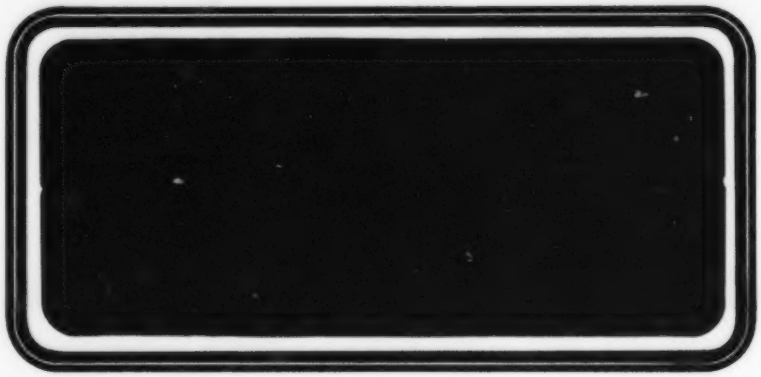

Canada Alberta

*The Canada-Alberta Forest Resource Development Agreement is a subsidiary agreement of the Canada-Alberta Economic and Regional Development Agreement, which provides coordination and cooperation between the governments of Alberta and Canada in areas of Alberta's economic development.*

*The Canada-Alberta Forest Resource Development Agreement is funded equally by the governments of Canada and Alberta, from April 1, 1984, to March 31, 1989.*

*Its primary objectives are to ensure the long-term availability of timber supplies; to optimize timber uses; and to contribute to the growth and diversification of Alberta's economy.*

*The Agreement comprises three programs: Reforestation; Applied research, technology transfer and opportunity identification; and Public information, evaluation and administration. These programs are managed by a joint Directorate and are implemented by Forestry Canada and the Alberta Forest Service.*

*L'Entente Canada-Alberta sur la mise en valeur des ressources forestières est auxiliaire à l'Entente Canada-Alberta sur le développement économique et régional, qui vise à assurer la coordination et la coopération des deux gouvernements relativement au développement économique de l'Alberta.*

*L'Entente Canada-Alberta sur la mise en valeur des ressources forestières est financée à parts égales par les gouvernements du Canada et de l'Alberta, et a cours du 1er avril 1984 au 31 mars 1989.*

*Ses objectifs principaux sont assurer la disponibilité à long terme de réserves de bois; optimiser leur utilisation; et contribuer à la croissance et la diversification de l'économie de la province.*

*L'Entente comprend trois programmes: Reboisement; Recherche appliquée, transferts de connaissances techniques et relevé des occasions; et Information, évaluation et administration. Ces programmes sont gérés par un Bureau de direction conjoint, et mis en oeuvre par Forêts Canada et le Service forestier de l'Alberta.*

For more information, please call or write:

Pour de plus amples informations, veuillez vous adresser à:


Forestry Canada
Northern Forestry Centre
5320 - 122 Street
Edmonton, Alberta
T6H 3S5
Telephone: (403) 435-7210

OR/OU Alberta Department of
Forestry, Lands & Wildlife
9915 - 108 Street
Edmonton, Alberta
T5K 2C9
Telephone: (403) 427-3583

# APPLICATION OF SCANNING AND IMAGING TECHNIQUES TO ASSESS DECAY AND WOOD QUALITY IN LOGS AND STANDING TREES

Forintek Canada Corp.[1]

1987

J.R. Hailey and P.I. Morris

This is a joint publication of Forestry Canada and the Alberta Forest Service pursuant to the Canada-Alberta Forest Resource Development Agreement

[1] Western Region, 6620 N.W. Marine Drive, Vancouver, B.C. B6T 1X2

Project # 1432-43

89-05230/

## DISCLAIMER

The study on which this report is based was funded in part under the Canada/Alberta Forest Resource Development Agreement.

The views, conclusions and recommendations are those of the authors. The exclusion of certain manufactured products does not necessarily imply disapproval nor does the mention of other products necessarily imply endorsement by Forestry Canada or the Alberta Forest Service.

(c) Minister of Supply and Services Canada 1988
Catalogue No.: FO 42-91/42-1988E
ISBN: 0-662-16265-X

Additional copies for this publication are available at no charge from:

Forestry Canada
Regional Development
5320 - 122nd Street
Edmonton, Alberta
T6H 3S5
Telephone: (403) 435-7210

or

Forestry, Lands and Wildlife
Forest Industry Development Division
108th Street Building
#930, 9942 - 108th Street
Edmonton, Alberta
T5K 2J5
Telephone: (403) 422-7011

## ABSTRACT

An extensive literature search focussed on the current capabilities of microwaves, ultrasonics, X-ray and gamma ray computed tomography (CT) and magnetic resonance (MR) to detect decay and wood quality of logs and standing trees. Microwaves are limited to shallow penetration and do not differentiate defects easily. Ultrasonics can differentiate a wide range of wood characteristics but have technical problems of acousitc coupling, resolution, response speed and equipment configuration. Computed tomography methods provide useful two-dimensional, gross density maps related to specific gravity and moisture distribution. Through interpretation they can detect and differentiate decay, knots, cracks, worm holes, annual rings, insect cavities, pruned branches, sapwood/heartwood boundaries, bark and resin pockets, blue stain, rocks and impregnation of liquor. Magnetic resonance imaging is the most promising technique because it provides a two-dimensional image of the chemical environment in the material as well as proton (1H) distribution. Several distinct signals are detected with MR, including the $T_1$ and $T_2$ relaxation times and permit correlation of these with the physical and chemical characteristics of wood. The same defects and internal charactertistics can be detected using MR as is possibl using CT. The experimental correlation studies of CT and MR with decay and wood quality characteristics have provided a PRELIMINARY evaluation of the techniques. The results confirmed and extended the claims made in the literature, and they indicate what future work needs to be done to develop and commercialize these techniques.

## ACKNOWLEDGEMENTS

The authors gratefully wish to acknowledge Millar Western Ltd. for supplying the experimental material and D.M. Wright for his assistance in compilation of the extensive figures.

TABLE OF CONTENTS


| | | Page |
|---|---|---|
| LIST OF TABLES | | vii |
| LIST OF FIGURES IN TEXT | | vii |
| LIST OF FIGURES IN APPENDIX | | viii |
| 1.0 | INTRODUCTION | 1 |
| 2.0 | OBJECTIVES | 2 |
| 3.0 | LITERATURE REVIEW | 3 |
| 3.1 | THE FIELD OF INTERNAL SCANNING AND IMAGING | 3 |
| 3.2 | MICROWAVES | 3 |
| 3.2.1 | Reflection | 6 |
| 3.2.2 | Refraction | 6 |
| 3.2.3 | Absorption | 6 |
| 3.2.4 | Delay | 6 |
| 3.2.5 | Depolarization | 6 |
| 3.3 | ULTRASONICS | 7 |
| 3.4 | X-RAYS, GAMMA RAYS AND NEUTRONS | 9 |
| 3.4.1 | X-ray Radiography | 9 |
| 3.4.2 | Neutron Radiography | 9 |
| 3.4.3 | X-ray and Gamma Ray Computed Tomography (CT) | 9 |
| 3.4.4 | Radiography and CT Summary | 11 |
| 3.5 | MAGNETIC RESONANCE (MR) | 11 |
| 3.5.1 | Magnetic Resonance Spectroscopy | 11 |
| 3.5.2 | Magnetic Resonance Imaging | 12 |
| 3.5.3 | Future Developments for MR Imaging | 13 |
| 3.5.4 | MR Summary | 13 |
| 4.0 | IMAGING DECAY AND WOOD QUALITY USING MR AND CT | 14 |
| 4.1 | EXPERIMENTAL PROCEDURES | 14 |
| 4.1.1 | Experimental Material | 14 |
| 4.1.2 | Decay Assessment | 14 |
| 4.1.3 | Moisture Content and Specific Gravity Determination | 16 |
| 4.1.4 | MR and CT Imaging | 24 |
| 4.1.5 | Photographic Imaging | 24 |
| 4.2 | RESULTS | 25 |
| 4.3 | DISCUSSION | 25 |
| 4.3.1 | Decay Assessment | 25 |
| | Decay Capability of Isolates | 25 |
| | Identification of Isolates | 25 |
| | Location of Wood-Rotting Basidiomycetes | 27 |
| | Comparison of CT and MR Images with Fungal Isolates | 28 |

TABLE OF CONTENTS, Contd.


| | | Page |
|---|---|---|
| 4.3.2 | Wood Quality Assessment | 29 |
| | Sound Knots | 30 |
| | Dead Knots | 30 |
| | Unsound Knots | 30 |
| | Compression Wood | 30 |
| | Stain | 31 |
| | Checks and Splits | 31 |
| | Pith | 31 |
| | Juvenile Wood | 31 |
| | Sapwood/Heartwood Boundary | 31 |
| | Extractives | 31 |
| | Specific Gravity | 32 |
| | Low Specific Gravity | 32 |
| | Moisture Pockets | 32 |
| | Wood Species | 32 |
| 4.3.3 | MR Imaging Using High Field Strength | 32 |
| 4.4 | CONCLUSIONS | 32 |
| 5.0 | APPLICATION OF IMAGING TO PRIMARY MILLS AND FORESTS | 34 |
| 5.1 | PRIMARY MILLS | 34 |
| 5.2 | FOREST APPLICATIONS OF INTERNAL SCANNING | 35 |
| 6.0 | RECOMMENDATIONS FOR FUTURE RESEARCH AND DEVELOPMENT | 37 |
| 7.0 | REFERENCES | 39 |
| 8.0 | ADDITIONAL REFERENCES | 47 |

## LIST OF TABLES

Table 1 Internal Defects and Wood Quality in Logs and Standing Trees

Table 2 Weight Loss and Identity for Wood-Rotting Basidiomycete Isolates

## LIST OF FIGURES IN TEXT

Figure 1. The electromagnetic spectrum

Figure 2. Pattern of sampling for mapping of fungus distribution in logs

Figure 3. This agar plate was inoculated with five chips from the sapwood of white spruce. Two basidiomycetes have grown out: Isolate WSa, unidentified, from the chip at the top left and Isolate WSb, Armillarea sp., from the chip at the top of the plate.

Figure 4. Five of these eight chips from the heartwood/sapwood boundary in trembling aspen have yielded Isolate TAa, a very slow growing fungus without the characteristic appearance of a wood rotting basidiomycetes: Phellinus tremulae.

Figure 5. Two of these chips, top and left, taken from the second heartwood sampling annulus in lodgepole pine, have yielded Isolate LPa, a fungus of basidiomycete appearance which does not produce characteristic clamp connections: Phellinus pini.

Figure 6. All eight of these chips from the heartwood of black spruce have yielded Isolate BSa, tentatively identified as Stereum sanguinolentum.

Figure 7. Three of these four chips from balsam fir heartwood have yielded Isolate BFa, Stereum sanguinolentum. The fourth chip has a non-basidiomycete fungus which was inhibited by the selective medium.

Figure 8. Three of these chips from alpine fir heartwood have yielded Isolate AFa, Stereum sanguinolentum. The fourth has a non-basidiomycete fungus which was inhibited by the selective medium.

Figure 9. All seven of these chips from the heartwood of white spruce have yielded Isolate WSb, easily identified as an Armillerea by the black root-like mycelial cords, rhizomorphs, characteristic of this genus.

LIST OF FIGURES IN APPENDIX


Figure I-1. UBC MR image of trembling aspen slice 1. TE = 26 msec.
Figure I-2. UBC MR image of trembling aspen slice 1. TE = 52 msec.
Figure I-3. UBC MR image of trembling aspen slice 1. TE = 78 msec.
Figure I-4. UBC MR image of trembling aspen slice 1. TE = 104 msec.
Figure I-5. UBC MR image of trembling aspen slice 1. TE = 130 msec.
Figure I-6. UBC MR image of trembling aspen slice 1. TE = 156 msec.
Figure I-7. MNI MR image of trembling aspen slice 1. TE = 30 msec.
Figure I-8. MNI MR image of trembling aspen slice 1. TE = 60 msec.
Figure I-9. MNI MR image of trembling aspen slice 1. TE = 90 msec.
Figure I-10. MNI MR image of trembling aspen slice 1. TE = 120 msec.
Figure I-11. MNI MR image of trembling aspen slice 1. TE = 150 msec.
Figure I-12. MNI MR image of trembling aspen slice 1. TE = 180 msec.
Figure I-13. MNI MR image of trembling aspen slice 1. TE = 210 msec.
Figure I-14. MNI MR image of trembling aspen slice 1. TE = 240 msec.
Figure I-15. MNI MR image of trembling aspen slice 1. TE = 30 msec., T2 8 echo summation, spot intensity definition.
Figure I-16. MNI MR image of trembling aspen slice 1. TE = 30 msec., T2 8 echo summation, line profile intensity definition.
Figure I-17. MNI MR image of trembling aspen slice 1. TE = 30 msec., T2 8 echo summation, 2X zoom, center of log.
Figure I-18. MNI MR image of trembling aspen slice 1. TE = 30 msec., proton density 8 echo summation.
Figure I-19. MNI MR image of trembling aspen slice 1. TE = 30 msec., proton density 8 echo summation, 2X zoom, center of log.
Figure I-20. MNI MR image of trembling aspen slice 1. TE = 30 msec., proton density 8 echo summation, 2X zoom, top right quadrant of log, line profile intensity definition.
Figure I-21. UBC CT image of trembling aspen slice 1.
Figure I-22. UBC CT image of trembling aspen slice 2.
Figure I-23. Color photograph of image plane for trembling aspen slice 1.
Figure I-24. Black and white photograph of image plane for trembling aspen slice 1.
Figure I-25. Color photograph of image plane for trembling aspen slice 2.
Figure I-26. Black and white photograph of image plane for trembling aspen slice 2.
Figure I-27. Location of fungus for trembling aspen slice 1A.
Figure I-28. Moisture content and specific gravity overlay for trembling aspen slice 1A.
Figure I-29. Location of fungus for trembling aspen slice 2A.
Figure I-30. Moisture content and specific gravity overlay for trembling aspen slice 2A.
Figure I-31. UBC MR image of balsam poplar slice 1. TE = 26 msec.
Figure I-32. UBC MR image of balsam poplar slice 1. TE = 52 msec.
Figure I-33. UBC MR image of balsam poplar slice 1. TE = 78 msec.
Figure I-34. UBC MR image of balsam poplar slice 1. TE = 104 msec.

LIST OF FIGURES IN APPENDIX, Contd.


Figure I-35. UBC MR image of balsam poplar slice 1. TE = 130 msec.
Figure I-36. UBC MR image of balsam poplar slice 1. TE = 156 msec.
Figure I-37. UBC CT image of balsam poplar slice 1.
Figure I-38. UBC CT image of balsam poplar slice 2.
Figure I-39. Color photograph of image plane for balsam poplar slice 1.
Figure I-40. Black and white photograph of image plane for balsam poplar slice 1.
Figure I-41. Color photograph of image plane for balsam poplar slice 2.
Figure I-42. Black and white photograph of image plane for balsam poplar slice 2.
Figure I-43. Location of fungus for balsam poplar slice 1A.
Figure I-44. Moisture content and specific gravity overlay for balsam poplar slice 1A.
Figure I-45. Location of fungus for balsam poplar slice 2A.
Figure I-46. Moisture content and specific gravity overlay for balsam poplar slice 2A.
Figure I-47. UBC MR image of lodgepole pine slice 1. TE = 26 msec.
Figure I-48. UBC CT image of lodgepole pine slice 1.
Figure I-49. UBC CT image of lodgepole pine slice 2.
Figure I-50. Color photograph of image plane for lodgepole pine slice 1.
Figure I-51. Black and white photograph of image plane for lodgepole pine slice 1.
Figure I-52. Color photograph of image plane for lodgepole pine slice 2.
Figure I-53. Black and white photograph of image plane for lodgepole pine slice 2.
Figure I-54. Location of fungus for lodgepole pine slice 1A.
Figure I-55. Moisture content and specific gravity overlay for lodgepole pine slice 1A.
Figure I-56. Location of fungus for lodgepole pine slice 2A.
Figure I-57. Moisture content and specific gravity overlay for lodgepole pine slice 2A.
Figure I-58. UBC MR image of alpine fir slice 1. TE = 26 msec.
Figure I-59. UBC MR image of alpine fir slice 1. TE = 52 msec.
Figure I-60. UBC MR image of alpine fir slice 1. TE = 78 msec.
Figure I-61. UBC MR image of alpine fir slice 1. TE = 104 msec.
Figure I-62. UBC MR image of alpine fir slice 1. TE = 130 msec.
Figure I-63. UBC MR image of alpine fir slice 1. TE = 156 msec.
Figure I-64. UBC CT image of alpine fir slice 1.
Figure I-65. UBC CT image of alpine fir slice 2.
Figure I-66. Color photograph of image plane for alpine fir slice 1.
Figure I-67. Black and white photograph of image plane for alpine fir slice 1.
Figure I-68. Color photograph of image plane for alpine fir slice 2.
Figure I-69. Black and white photograph of image plane for alpine fir slice 2.

LIST OF FIGURES IN APPENDIX, Contd.


Figure I-70. Location of fungus for alpine fir slice 1A.
Figure I-71. Moisture content and specific gravity overlay for alpine fir slice 1A.
Figure I-72. Location of fungus for alpine fir slice 2A.
Figure I-73. Moisture content and specific gravity overlay for alpine fir slice 2A.
Figure I-74. UBC MR image of balsam fir slice 1. TE = 26 msec.
Figure I-75. UBC MR image of balsam fir slice 1. TE = 52 msec.
Figure I-76. UBC MR image of balsam fir slice 1. TE = 78 msec.
Figure I-77. UBC MR image of balsam fir slice 1. TE = 104 msec.
Figure I-78. UBC MR image of balsam fir slice 1. TE = 130 msec.
Figure I-79. UBC MR image of balsam fir slice 1. TE = 156 msec.
Figure I-80. UBC CT image of balsam fir slice 1.
Figure I-81. UBC CT image of balsam fir slice 2.
Figure I-82. Color photograph of image plane for balsam fir slice 1.
Figure I-83. Black and white photograph of image plane for balsam fir slice 1.
Figure I-84. Color photograph of image plane for balsam fir slice 2.
Figure I-85. Black and white photograph of image plane for balsam fir slice 2.
Figure I-86. Location of fungus for balsam fir slice 1A.
Figure I-87. Moisture content and specific gravity overlay for balsam fir slice 1A.
Figure I-88. Location of fungus for balsam fir slice 2A.
Figure I-89. Moisture content and specific gravity overlay for balsam fir slice 2A.
Figure I-90. UBC MR image of black spruce slice 1. TE = 26 msec.
Figure I-91. UBC MR image of black spruce slice 1. TE = 52 msec.
Figure I-92. UBC MR image of black spruce slice 1. TE = 78 msec.
Figure I-93. UBC MR image of black spruce slice 1. TE = 104 msec.
Figure I-94. UBC MR image of black spruce slice 1. TE = 130 msec.
Figure I-95. UBC MR image of black spruce slice 1. TE = 156 msec.
Figure I-96. UBC CT image of black spruce slice 1.
Figure I-97. UBC CT image of black spruce slice 2.
Figure I-98. Color photograph of image plane for black spruce slice 1.
Figure I-99. Black and white photograph of image plane for black spruce slice 1.
Figure I-100. Color photograph of image plane for black spruce slice 2.
Figure I-101. Black and white photograph of image plane for black spruce slice 2.
Figure I-102. Location of fungus for black spruce slice 1A.
Figure I-103. Moisture content and specific gravity overlay for black spruce slice 1A.
Figure I-104. Location of fungus for black spruce slice 2A.
Figure I-105. Moisture content and specific gravity overlay for black spruce slice 2A.

LIST OF FIGURES IN APPENDIX, Contd.


Figure I-106. UBC MR image of white spruce slice 1. TE = 26 msec.
Figure I-107. UBC MR image of white spruce slice 1. TE = 52 msec.
Figure I-108. UBC MR image of white spruce slice 1. TE = 78 msec.
Figure I-109. UBC MR image of white spruce slice 1. TE = 104 msec.
Figure I-110. UBC CT image of white spruce slice 1.
Figure I-111. UBC CT image of white spruce slice 2.
Figure I-112. Color photograph of image plane for white spruce slice 1.
Figure I-113. Black and white photograph of image plane for white spruce slice 1.
Figure I-114. Color photograph of image plane for white spruce slice 2.
Figure I-115. Black and white photograph of image plane for white spruce slice 2.
Figure I-116. Location of fungus for white spruce slice 1A.
Figure I-117. Moisture content and specific gravity overlay for white spruce slice 1A.
Figure I-118. Location of fungus for white spruce slice 2A.
Figure I-119. Moisture content and specific gravity overlay for white spruce slice 2A.

## 1.0 INTRODUCTION

The ultimate utilization of the major species in Alberta will require minimization of the impact of defects on solid wood products or re-constituted wood products produced. The products must be durable, serviceable and dimensionally stable. Of considerable importance are the major hardwood species: trembling aspen [Populus tremuloides (Michx.)] and balsam poplar [Populus balsamifera (L.)]. Commercial use of these species has met with limited success. One major cause is the widespread existence of internal defects and characteristics including wet pockets, pocket rot, incipient decay and stain. These are often found in wood of these species, which appears sound upon external examination. Also of importance are the major softwood species: lodgepole pine [Pinus contorta (Dougl.) var. latifolia (Engelm.)]; alpine fir [Abies lasiocarpa (Hook.) Nutt.]; balsam fir [Abies balsamea (L.) Mill.]; black spruce [Picea mariana (Mill.) BSP]; and white spruce [Picea glauca (Moench) Voss var. albertiana (S.Brown) Sarg]. These species are used for lumber, solid wood products and re-constituted wood products such as oriented strandboard and pulp and paper. Knowledge of the moisture distribution and chemical composition as well as the nature of defective or abnormal regions in wood will assist the development of better utilization techniques for extracting maximum value from logs, chips and lumber. The identification of such characteristics as wood density, wet pockets, incipient decay, pocket rot, knots, compression wood and sapwood, heartwood and juvenile wood boundaries will be of considerable value in the timely use of computer optimization programs for log and lumber breakdown. Application of this knowledge to standing timber should lead to improved stand management techniques to provide increased growth and increased wood quality.

The use of internal scanning and imaging technology has good potential to identify and spatially locate the various characteristics already discussed. The techniques of X-ray computed tomography (CT), magnetic resonance (MR) imaging, ultrasonics and microwaves are four which deserve investigation. Although these techniques are in varying stages of development, they should be applicable to logs and lumber in locations where space limitations are not a problem. These internal scanning techniques should eventually be applicable to standing trees with the attendant reduction in equipment size and optimization of parameters which will yield the most appropriate information for the forester.

## 2.0 OBJECTIVES

1. To identify and evaluate the use of and potential opportunities for internal scanning and imaging technologies to assess decay and wood quality in logs and standing trees for the principle species of Alberta through a comprehensive literature review.

2. To produce and analyze images using X-ray Computed Tomography and Magnetic Resonance imaging to demonstrate the potential for scanning and imaging decay and wood quality in logs and standing trees for the principle species of Alberta. To identify the parameters used for each species considered.

3. To evaluate the scanning and imaging technologies in terms of their potential application in the primary mills (sawmills, pulpmills, and panelboard plants) with an estimate of the costs involved and the potential increases in productivity and savings.

4. To identify opportunities for further research, developments and applications or adaptations by the Alberta forest industries and R & D establishments of the methods and equipment reviewed.

# 3.0 LITERATURE REVIEW

## 3.1 THE FIELD OF INTERNAL SCANNING AND IMAGING

In theory, any technique which provides a signal that varies in response to the internal characteristics of logs or standing trees can provide the necessary information for a two dimensional image. Examination of the electromagnetic spectrum (Figure 1) shows a range in frequencies from $10^3$ Hz to $10^{25}$ Hz. Signals from the external and/or internal characteristics of materials can be produced over this frequency range. This review will concentrate on four window areas (Figure 1) which can give a signal related to the internal characteristics of wood: microwaves (300 MHz to 300 GHz); ultrasonics (20 kHz to 500 MHz); X-rays ($10^{18}$ Hz to $10^{20}$ Hz, which include X-rays and Gamma rays); and magnetic resonance (MR) (1 KHz to 50 MHz).

The internal characteristics that are useful to identify are shown in Table 1. Techniques developed for the detection of decay in wood poles are described in a number of manuals and review articles (Stott, 1969; Goodell and Graham, 1983; Morris and Friis-Hansen, 1984; and Smith, 1984). Non-imaging techniques range from picking, visual evidence, drilling, torque measurement, resonant sounding, colour reactions, moisture content, impact resistance strength testing (pilodyn), pulsed audio signal-electrical resistance (shigometer), sonic velocity (pol-tek), acoustic dampening, acoustic vibration, to X-rays or gamma rays, $CO_2$ detection, sniffer dogs, mechanical impedance, culturing of fungi, microscopy, ultrasonic (Purl), electrical resistance, strength tester (PEST), to name the majority of reported techniques. Techniques which lend themselves to mapping the location of internal decay will be described in the following sections (i.e., ultrasonics and X-rays).

There have also been a number of overviews on scanning for defect and wood quality detection for the solid wood product industries, including: Anon, 1984; Mayer, 1985; Szymani, 1979; Szymani and McDonald, 1981; Szymani, 1985; Lee, 1958. Some of the techniques are offshoots from the medical scanning field (Mayer, 1985; Burgess, 1985). These techniques cover the fields of video scanning, electrical scanning for moisture content, laser and fibre optic scanning, sub-sonic, sonic and ultrasonic vibrations, microwaves, X-rays, positron emission tomography (PET), electron spin resonance (ESR), neutron scanning, magnetic resonance (MR) imaging and optical methods. Again, the methods lending themselves to spatial location of internal wood characteristics will be covered in the following sections (i.e., microwaves, ultrasonics, X-ray computed tomography and MR imaging).

## 3.2 MICROWAVES

Microwaves have a frequency from 300 MHz to 300 GHz and a corresponding wavelength in air from 1 m to 1 mm, respectively. The wavelengths would be 1/2 to 1/5 as long in wood, depending on the dielectric constant of wood. Microwaves have different propagation phenomena - reflection, refraction, absorption, delay and depolarization. Information can be generated for both phase and amplitude.

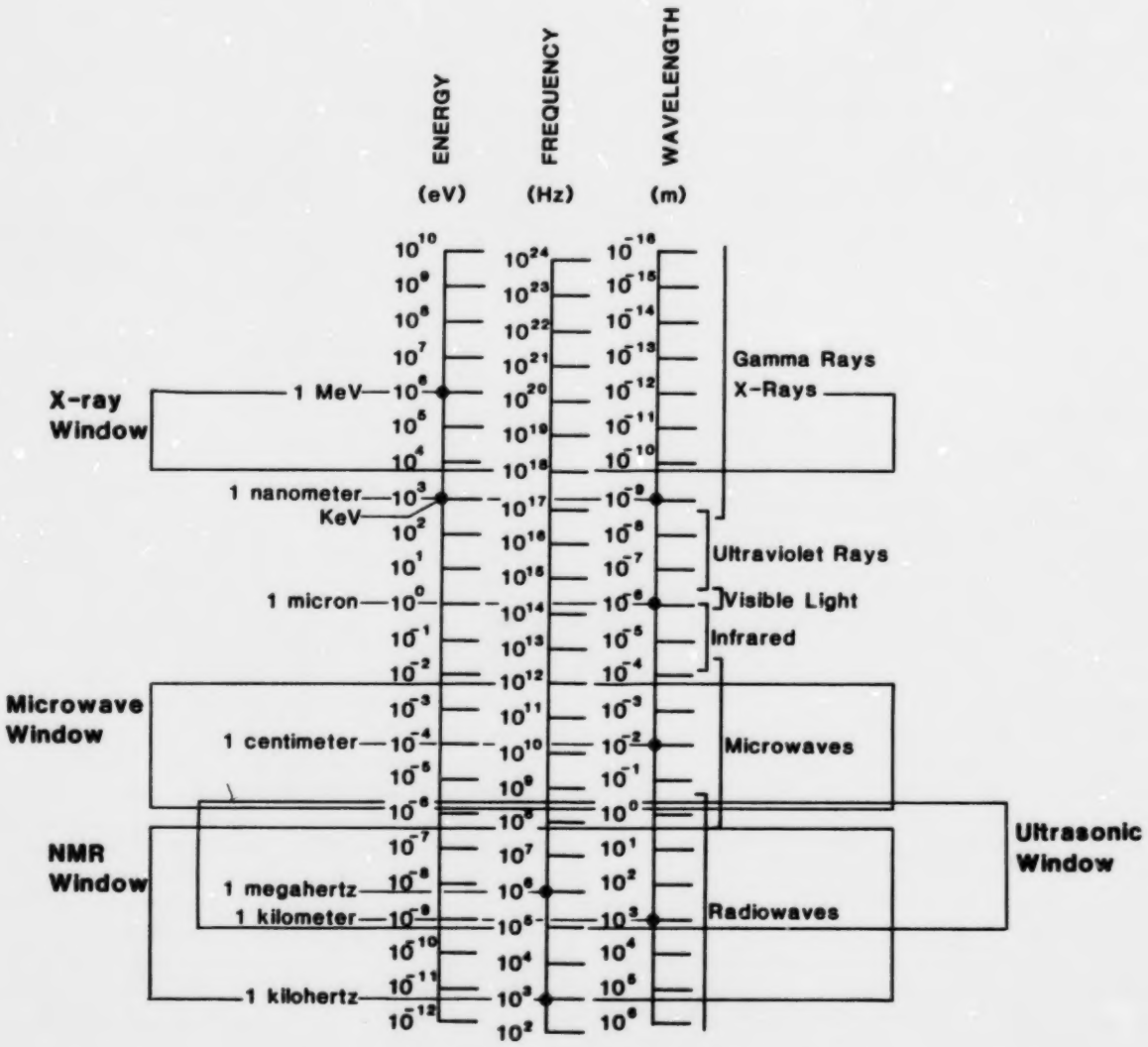


The Electromagnetic Spectrum

**Figure 1.**

Table 1

Internal Defects and Wood Quality in Logs and Standing Trees

| | | |
|---|---|---|
| - | sound knots* | dead knots* |
| - | unsound knots* | |
| - | compression wood* | tension wood |
| - | worm holes | grub holes |
| - | decay* | rot* |
| - | incipient decay* | stain* |
| - | spiral grain | checks* |
| - | splits* | pitch pockets |
| - | cross grain | pith* |
| - | bark pockets | |
| - | specific gravity* | low density* |
| - | juvenile wood* | sapwood/heartwood boundary* |
| - | extractives* | wood species* |
| - | moisture pockets* | |
| - | foreign objects - rocks, metal, etc. | |

*Indicates defects present in experimental sample log sections.

### 3.2.1 Reflection

An electromagnetic wave impinging on the interface between air and a dielectric interface has some of the energy reflected. The amount of energy reflected depends on the dielectric constants of the two materials, the angle of incidence and the polarization of the wave.

### 3.2.2 Refraction

The energy that is not reflected is transmitted into the other material. The wave is usually refracted at the interface. The velocity of the refracted wave is inversely proportional to the refractive index of the material. The refractive index in turn is the square root of the dielectric constant of the material. When the wave passes the interface, it follows the angle of transmission which is dependent on the refractive indexes of the materials. This change of direction must occur to ensure phase continuity across the boundary.

### 3.2.3 Absorption

Dielectric materials usually absorb electromagnetic energy and convert it to heat. The amount of absorption depends on the material and to some degree on the frequency. The wave thus loses energy as it passes through the dielectric material. Although many materials exhibit low loss factors, water in either solid or gaseous form leads to increased loss. Absorption is usually a linear effect dependent on the distance travelled.

### 3.2.4 Delay

Since the velocity of the wave in a material varies with the dielectric constant, a delay in the wave propagation occurs when compared to its propagation through the same distance in a vacuum. This delay is proportional to the refractive index and the distance travelled.

### 3.2.5 Depolarization

When a planar wave impinges on an object of arbitrary shape, the surfaces may not always correspond to the polarization planes of the wave. The reflected wave may then have a polarization which differs from the incident wave; it is thus depolarized. This phenomenon can also occur when the wave propagates through an anisotropic or inhomogeneous material.

The field of microwaves is the least developed and requires more work to determine how promising it will be for application to internal scanning of logs and standing trees. Using the previously described microwave propagation properties, work has concentrated on the detection of such wood characteristics as density, moisture content, grain direction, shape, thickness, surface conductivity, decay, holes, knots and dielectric constant (Szymani and McDonald, 1981; Szymani, 1979; Szymani, 1985; Bergh, 1985; Juvonen, 1985; King *et al.*, 1985). Microwaves are unable to penetrate deeply into conductors, making them more suited to applications using lumber than to applications using logs or standing trees. In addition, the differentiation of defects smaller than the wavelength are difficult even in lumber sized pieces.

## 3.3 ULTRASONICS

Ultrasonics refers to the generation, propagation, detection and use of ultrasound (sound with a frequency between 20 KHz and 500 MHz - Figure 1). Because the propagation of ultrasound is basically a mechanical phenomenon, it has been used frequently for the non-destructive evaluation of internal characteristics in wood (Stott, 1969; Goodell and Graham, 1983; Morris and Friis-Hansen, 1984; SMith, 1984; Szymani, 1985; Lee, 1958; Miller et al., 1965; Parrott, 1965; Anon., 1983; Holland and Heath, 1983; Kristiansen, 1985; Mayer, 1985; Pellerin et al., 1986; Arita et al., 1986; Szymani, 1979; Szymani and McDonald, 1981).

Ultrasonic waves (longitudinal or transverse) can be propagated in any elastic body with the form of the wave dependent on the elastic properties of the medium. Longitudinal waves (compression waves) are created by displaced particles vibrating parallel to the direction of wave propagation. The velocity is dependent on Young's modulus, Poisson's ratio and the density. For transverse waves (shear waves) the displaced particles vibrate perpendicular to the direction of wave propagation. The velocity is dependent on the modulus of rigidity and the density. Longitudinal waves have a high velocity in most media with the wavelengths being very short compared to the cross-sectional area of the transducer producing the waves. This allows focussing of the energy into a sharp beam. Transverse waves, on the other hand, have a velocity about half that of the longitudinal waves and a similarly shorter wave length. The shorter wavelength makes the transverse waves more sensitive to small inclusions and results in internal scattering of the waves.

Ultrasonic waves may be subjected to reflection, refraction or mode conversion when the waves propagated in one medium reach an interface with another medium. Mode conversion is the changing of longitudinal waves into transverse waves and visa versa. Each medium has a characteristic impedance, which is given as the product of the wave velocity and the density, and helps determine the transported waves' energy intensity. An incident wave impinged on a plane interface at other than a zero angle of incidence will give both longitudinal and transverse reflected and transmitted waves. Internal differences in density and velocity due to inclusions (defects) give rise to changes in the wave energy intensity and thus information about the type and location of defects.

There are at least five different ways ultrasonic testing can be done. One way is through transmission requiring a transmitter and a receiver. A defect or flaw reflects some of the energy, causing a reduction in amplitude. For the other methods, the transmitter and receiver are one and the same and use echoes to detect changes inside a material. Echo ranging uses a straight beam which, if a defect or flaw is present, echoes the beam back while the end of the work piece creates a back echo. Other techniques use variations of this same principle.

One major problem with ultrasonics for imaging logs and standing trees is the acoustic coupling between the transducer (a piezoelectric crystal) and the wood. The characteristic impedance of air (0.0004 $kg/m^2$) is about 1/5000 that of wood (1.7 $kg/m^2$ for pine to 3.5 $kg/m^2$ for oak) giving rise to an almost

total loss of energy transmission. This can be resolved by ensuring that no air gap exists between transducer and the wood surface. To overcome this difficulty, water has been used as an acoustic coupling medium, since its characteristic impedance (1.48 $kg/m^2$) is closer to that of wood. This technique has led to the spatial location and identification of such internal wood characteristics as knots, cross grain, rot, holes (greater than 3/4 in.), pitch pockets, bark inclusions, pith, wane, and torn grain in lumber (Kristiansen, 1985; Mayer, 1984; Szymani, 1979; Szymani and McDonald, 1981; Szymani, 1985) and in logs (Mayer, 1984). Normal variations in moisture and specific gravity are not readily identified by this approach.

Work in the area of rot detection and spatial location has occurred with some success (Arita et al., 1986; Morris, 1986). The method used by Arita et al. (1986) uses propagation time and signal decay (attenuation) between a transducer and receiver. To detect sapwood decay the transducer and receiver are first placed across the diameter at a healthy location on the post to give a propagation time for a reference value. The propagation time is then measured through the diameter eight times at equally spaced intervals around the post at the location of interest (usually at groundline). The propagation time is then measured for each quadrant with the transducer/receiver placed at 90 degrees to each other. For heartwood decay the transducer is placed at one location and the receiver is moved stepwise around the circumference to pick up the difference in propagation time. This approach is tedious; however, results are promising.

Two independent lines of research in the United Kingdom have recently come up with experimental scanning devices for imaging decay in wooden poles and railway ties, respectively (Morris, 1986). The former evaluates attenuation of an ultrasonic pulse across the pole between three transmitter and 27 receiver positions. The presence or absence of a threshold level for the signal denotes sound or decayed wood respectively between the transmitter and receiver. The 27 positive or negative readings are used to create a computerized tomogram of the decay. Several independent evaluations (one of which was carried out by P.I. Morris) showed that the device shows a great deal of promise but requires fine tuning. Refinement of the device is currently underway in the U.K. and it may be possible to obtain a modified version in the near future.

The second British device analyzes the wave form created in a tie by an impact from a hammer. It is claimed that the analysis can detect the location and extent of defects within the tie. This device is being developed by Biokil Chemicals Ltd. under contract to British Rail as part of a remedial treatment and a maintenance program.

Ultrasonics show good promise for imaging in the future because of their ability to detect a wide range of wood characteristics. For logs and standing trees the acoustic coupling problems must be better resolved. Resolution and response speed must also be improved.

## 3.4 X-RAYS, GAMMA RAYS AND NEUTRONS

### 3.4.1 X-ray Radiography

The X-ray window (Figure 1) for looking at wood includes both X-rays, gamma rays and neutrons. X-rays characteristically have short wavelengths between $5 \times 10^{-9}$ and $10^{-12}$ meters. The X-ray tubes are operated at a potential of between 6 KeV and 1 MeV. For radiography, an X-ray tube is used as a source of X-rays and an image receptor--photographic film, fluorescent screen, TV screen or scintillographic system--is used to detect changes in attenuation (decay) as the rays pass through the object. The projection image of the material being examined is the sum of the transmitted energy through the object. The horizontal location of any included defects can be determined; however, the vertical spatial location cannot be determined from a single transmission. Work has been done to detect decay, insect damage, density profiles, holes and knots using radiographic techniques (Szymani, 1979; Szymani and McDonald, 1981; Szymani, 1985; Birring and Smith, 1985; Truman, 1953; Gardner et al., 1980; Thornton et al., 1980; Liu et al., 1984; Burgess, 1985; Nystrom, 1985; Solberg, 1985; Harbich, 1984). A practical application of radiography in the forest industry is the TINA log quality measuring system in Sweden (Nystrom, 1985). The transmitted intensity at two diameters at right angles is used to place the logs into quality classes. Density variations and knot locations determine the class. However, a precise two dimensional spatial location of included wood characteristics is not possible through this technique.

### 3.4.2 Neutron Radiography

Neutron radiography (Solberg, 1985; Szymani, 1979; Szymani and McDonald, 1981) is similar to X-ray radiography but can penetrate a greater thickness of more dense material with less scattering. Even greater difficulty in obtaining a two dimensional image is present since it examines the total mass content as opposed to mass content along specific rays as given by X-ray or gamma ray methods. This technique has proven useful in measuring moisture content in bulk materials, consistency of pulp slurries, density, thickness, flaws, cracks, voids and inclusions.

### 3.4.3 X-ray and Gamma Ray Computed Tomography (CT)

Computed tomography is one of the most significant advances in X-ray imaging, since it allows the internal structure of an object to be reconstructed from multiple projections of the object. A thin cross section of the object is scanned with a wide fan X-ray or gamma ray beam and the transmitted radiation detected. The beam is rotated through 360 degrees and the resulting photon density data is reconstructed into a two dimensional image using an appropriate algorithm. Computed tomography imaging is not confined to the wood products industry (Allan, 1984; Hartley, 1986). However, CT imaging has been used to study wood all over the world, particularly with logs or standing trees.

These studies began using medical scanners to determine the potential of this technique (Burgess, 1985; Hailey et al., 1985; Schmidt, 1978; Asplund and Johansson, 1984; Benson-Cooper, 1982; Hattori, 1985; Funt and Bryant, 1984;

Taylor et al., 1984; Wagner and Taylor, 1985; Taylor, 1980; Birring and Smith, 1983; Sorenson, 1986). These studies have demonstrated that internal defects and wood characteristics such as decay, knots, cracks, worm holes, annual rings, insect cavities, pruned branches, sapwood/heartwood boundary, bark and resin pockets, blue stain, rocks, moisture distribution and extent of impregnation liquor can be detected and differentiated. The 1 mm resolution of current imaging systems was noted as being more than required for industrial forest products application. The time needed to collect the data and to reconstruct the image is currently too long for potential on-line applications. The high cost of medical scanners (in excess of $1 million) was considered to be prohibitive. Radiation hazard, life expectancy of the X-ray tubes, the need for highly qualified personnel, and availability of highly complex computer programs to make use of the internal information for maximizing recovery were some of the additional problems to be solved before medical types of scanners can be used in industrial applications.

There are three other areas of interest in imaging using X-ray CT. To address the problem of how to take advantage of the internal information from CT, the Japanese have looked at the determination of grain orientation to maximize value recovery in lumber (Noguchi, 1985; Tochigi, 1983). Soft X-rays were used to determine the grain orientation and knot location in test logs. A computer simulation program was used to generate an optimum sawing solution. This system is still too expensive for adoption by Japanese industry.

The Japanese have developed a portable CT scanning system for use on standing trees (Onoe et al., 1983; Fox, 1983; Onoe, 1986; Nakamura, 1984). The scanner has three columated X-ray beams at eight degrees apart with projection data taken every two degrees around the circumference of the tree to obtain a two dimensional image of the tree. Decay, tree rings, knots and various other internal defects can be determined with adequate resolution. However, a weight of 50 kg, a scan time of 10-1/2 hours, and the inability to produce on-the-spot pictures, make the present system unacceptable for frequent use.

The other main development is in Germany where a portable gamma ray CT scanner has been used to reasonably successfully measure decay in standing trees (Habermehl, 1982a and 1982b). This device uses a single source and detector on opposite sides of the tree. The attenuation of the beam is measured for the entire thickness of the stem at one location. The device then moves the source/detector along a coordinated parallel path until the entire diameter has been scanned. The device is then turned through a small angle and the next profile recorded. A complete profile of the cross section is built up. The data are collected and the reconstruction is completed in the laboratory. A three dimensional representation of the two dimensional absorption coefficient map is created to allow ease of interpretation. The four classifications of decay require some subjective interpretation from the created image. Resolution required improvement to identify small areas of decay. In addition, a semi-portable rapid data collecting system was described using a wide fan beam source and a 71 detector array, rotated around the circumference every eight degrees. In addition to the decay application it is hoped some correlations can be developed between the absorption coefficient and the chemical composition of the wood.

### 3.4.4 Radiography and CT Summary

Computed tomography is a dramatic improvement over radiographic techniques which can only give a one dimensional spatial location of internal wood characteristics. Computed tomography provides a two dimensional reconstructed gross density map utilizing the absorption coefficient of the wood cross section. It does detect and differentiate the following internal defects and wood characteristics: decay, knots, cracks, worm holes, annual rings, insect cavities, pruned branches, sapwood/heartwood boundary, bark and resin pockets, blue stain, rocks, moisture distribution, and impregnation of liquor. The utilization of CT scanners in the sawmill appears to be at least two years away. The high cost of CT scanners ($0.6 to $2 million) must be reduced. The refinement of portable scanners is continuing in Japan and Germany. The radiation hazard must be protected against.

## 3.5 MAGNETIC RESONANCE (MR)

The magnetic resonance window makes use of the low-energy, radio frequency band of the electromagnetic spectrum (Figure 1) from 1 KHz to 800 MHz. The principle of MR (Fullerton, 1982; Pykett et al., 1982; Portugal, 1984) begins with the object to be studied being placed in a very uniform magnetic field. Those nuclei within the object with a magnetic moment align themselves to the external magnetic field. The magnetic moment of the nuclei precess about the magnetic field with an angular frequency called the Larmor frequency. This frequency is dependent on the field strength and the magnetogyric constant which is characteristic of the specific nucleus under study. Nuclei with a high magnetogyric constant ($^{1}H$ and $^{19}F$) lend themselves to imaging and spectroscopy, while those with a lower constant ($^{13}C$ and $^{31}P$) can be used for spectroscopy. If the object is then irradiated with a radio frequency (RF) wave at the resonant frequency, the magnetization will be rotated out of the original plane. When the RF wave ceases, the magnetization realigns itself with the original plane. The two characteristic relaxation phenomona are $T_1$ (the spin-lattice relaxation time) where the perturbed nuclei realign themselves with the lattice structure, and $T_2$ (the spin-spin relaxation time) where the perturbed in-phase spins dephase with respect to one another. The importance of these two relaxation times is that they provide information about the chemical environment in the vicinity of the protons. There is no similar analogy with X-rays.

### 3.5.1 Magnetic Resonance Spectroscopy

Part of the basis for scanning or imaging of logs or standing trees using MR is the characteristic relaxation time of different internal wood characteristics which can be obtained from spectroscopic studies. Both the spectroscopy and imaging of wood to date look at 1H protons because of their relative abundance and high magnetogyric constant. A number of spectroscopic studies examined the moisture content of wood and/or pulp using an MR technique (Magnusson et al., 1972; Nanassy, 1973, 1974, 1976, 1978). To obtain an accurate estimate, the weight of the sample was required. Subsequent studies looked at water flow and diffusion in wood (Parker, 1985; Peemoeller et al., 1985; Gummerson et al., 1979; MacGregor, 1983). Further

studies have looked at understanding the location of the water in the wood and defining the relaxation times (Riggin et al., 1979; Byrne et al., 1986; Menon et al., 1987; Johansson, 1985; Hailey et al., 1985). One of the more definitive studies (Menon et al., 1987) has shown that for Douglas-fir and western red cedar there are three components to the $T_2$ relaxation time which have been anatomically confirmed. These components are: water in the cell walls, water in the latewood tracheids and ray cells, and water in the earlywood tracheids. Because water in the cell walls should be most influenced by the chemical environment, the identification and eventual imaging of this component should lead to better identification of wood characteristics.

The absolute moisture content of wood can be determined from the free induction decay when combined with a knowledge of the chemical composition of the wood. The fibre saturation point can be determined from a single $T_2$ measurement on the sapwood. Follow-up work has been underway during the past year and has resulted in further collaborative evidence as to the location of the water components. A reduction in $T_2$ value due to the presence of decay has also been shown. In addition, some differences in $T_1$ between species have been indicated. The spectrometer studies above all can enhance the interpretation of MR images (Menon et al., 1987; Hailey et al., 1985).

A further area of interest is the solid signal from the cell walls. The MR spectroscopy of the lignin and cellulose may lead to applications in the pulp and paper field. Work with bean plant cell walls (Taylor et al., 1983; MacKay et al., 1982) has characterized cellulose and pectin. Thus, the characterization of cellulose, hemicellulose and lignin should also be possible with the cell walls of wood. This could lead to rapid identification of wood quality since it relates to the chemical makeup.

### 3.5.2 Magnetic Resonance Imaging

Magnetic resonance imaging uses the same basic process as spectroscopic studies (Burgess, 1985; Pykett et al., 1982; Fullerton, 1982; Portugal, 1984; Aronson, 1984). The addition of a one dimensional field gradient coil across the object allows a projection profile to be created in the perpendicular direction. The gradient direction is rotated in increments to cover 180 degrees. The data intensity profiles of these projections is used to reconstruct a map of the protons in the object. By using different RF pulse sequences, $T_2$ and $T_1$ maps can also be obtained. Several studies have investigated MR imaging of wood (Hailey et al., 1985; Asplund and Johansson, 1984; Johansson, 1985; Burgess, 1985; Hall et al., 1985; Kucera et al., 1985; Wang and Chang, 1985). The technique can detect the presence of the following wood characteristics: knots, sapwood/heartwood boundary, decay, moisture pockets, worm holes, shake, annual rings and juvenile wood. Potential future applications of the technique are in wood drying, wood preservation and plant pathological studies. Problems for on-line application include the scanning time, which is currently up to tens of minutes long, the high cost of the scanners (over $1,000,000), the immobility of the systems, and lack of detailed studies on the fundamental parameters involved.

### 3.5.3 Future Developments for MR Imaging

The direction of research (Anon., 1986a, b, c, d and e) is helping to make MR a more effective tool for physiological characterization. Of particular interest for future wood products applications are the developing high-speed imaging techniques. Work is also being done on flow imaging, which is also of importance because fast imaging sequences are required to characterize flow. The consensus is that practical MR imaging of a single slice will be done in a 30 millisecond interval, making the technique practical for fast full characterization of an entire log, at some time in the near future. Other developments include the use of ultra-low field magnets (less than 0.02 Tesla) which reduce the cost of such a system. Work is being done by the major MR imaging companies (Picker, Phillips, Siemens etc.) on various image reconstruction techniques which will more completely define the inherent characteristics of the material being imaged, particularly $T_1$ and $T_2$. The M.V. Phillips (Holland) group showed interest last August at the Fifth Annual Meeting of the Sociey of Magnetic Resonance in Medicine conference in application of MR to forestry. Magic angle and chemical shift imaging may help to more fully define the chemical characteristics of the material being studied.

### 3.5.4 MR Summary

Magnetic resonance is such a promising technique for the forest industry because it detects the effect of the physical and chemical environment on the proton (1 H) distribution. Magnetic resonance spectroscopy allows the non-destructive determination of the moisture content of wood. The fibre saturation point can be determined from a single sapwood measurement.

Magnetic resonance also allows correlation of the high resolution measurements of the relaxation times ($T_1$ and $T_2$) with the physical and chemical characteristics of wood for optimizing imaging. One of the relaxation times ($T_1$) may allow some separation of species.

Magnetic resonance imaging allows reconstruction of a two dimensional image of any plane through wood. Proton density, and $T_1$ and $T_2$ maps of the internal physical and chemical characteristics can be reconstructed. The following defects and internal characteristics can be detected: knots, sapwood/heartwood boundary, decay, moisture distribution and pockets, worm holes, shake, annual rings and juvenile wood. The log scan times currently required (many minutes) may soon be reduced to tens of milliseconds using high speed imaging techniques. The high cost may be reduced dramatically by use of lower magnetic field magnets. This in turn would reduce the size of the equipment.

Mill applications using some of the basic MR parameters could occur within the next few years. Application of two or three dimensional MR imaging of whole logs in sawmills is five years or longer away.

# 4.0 IMAGING DECAY AND WOOD QUALITY USING MR AND CT

## 4.1 EXPERIMENTAL PROCEDURES

### 4.1.1 Experimental Material

A two-foot log segment of each of the seven Alberta species listed in the Introduction were obtained in early July, 1986, courtesy of Millar Western Industries Inc. from their logging area in the Whitecourt Forest District. Each segment was freshly bucked with some decay present and was approximately 12 inches in diameter. The segments were double-wrapped in plastic to retain the moisture that was present. Within a week of arrival at Forintek, after removing four inches of trim, a one-inch disc was removed from each end of the log segments for carrying out decay assessment. These discs were labelled Slice 1A and Slice 2A. The decay assessment was to allow correlation with MR and CT images to be subsequently obtained. The remainder of the log segments were then heavily wrapped in plastic and stored in a controlled environment chamber at 26 percent relative humidity to minimize moisture loss.

### 4.1.2 Decay Assessment

Although visible evidence of decay such as discolouration, softening and shrinkage was readily discernible in most of the logs under study the absence of these diagnostic features in some areas does not necessarily preclude the presence of wood-rotting basidiomycetes and reduction in strength properties. These fungi can frequently be isolated several centimeters from the edge of the visibly decayed area.

It may also be the case that areas of timber with discolouration suggestive of early stages of decay may be due to wound responses of the tree rather than fungal attack.

Since MR spectroscopy can detect the effect of solutes in wood on the MR parameters, there may be an effect from fungal metabolites, in particular radical cations and other highly reactive chemical species involved in decay on these same parameters. The concentrations of these metabolites may vary with the stage of decay and may help to explain variations in the MR spectrum.

In order to confirm the preliminary application of scanning techniques for decay detection it was necessary to assess the extent of colonization by the wood-rotting basidiomycetes (WRB).

The two 1 inch thick slices, cut from each end of each log adjacent to the positions to be scanned, were stored in plastic bags in a refrigerator until they were sampled. The sampling technique was originally developed for determining fungal distribution in wood poles (Morris, Dickinson and Levy, 1984). It accounts for any variation in size or shape of roundwood while permitting accurate location of fungi isolated.

Small chips of timber were removed at 20 mm intervals around sample "annuli" spaced 20 mm apart, working in two directions away from four radii at 90° to each other (see Figure 2). One of the four radii is arbitrarily designated

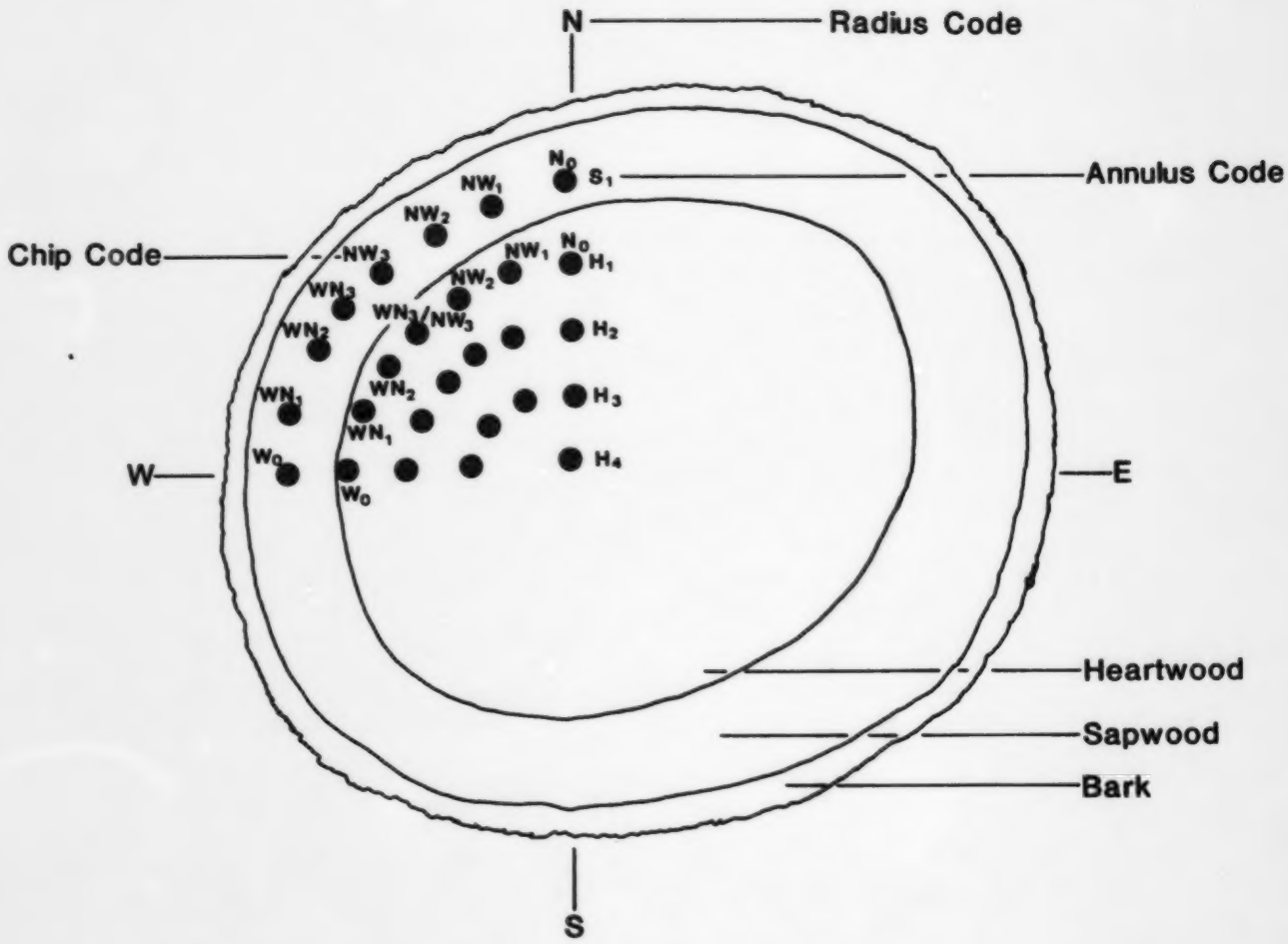


**Figure 2. Pattern of sampling for mapping of fungus distribution in logs.**

north and the others are consequently south, east and west. The sample chips were identified by their position with respect to these four radii. The chips at the four radii were given the subscript $N_o$, $S_o$, $W_o$ or $E_o$. The chips 20 mm either side were NE, NW, WN, etc., subscript 1 and the next either side were subscript 2, etc. Where the sets of samples, e.g. NW and WN, approached one another, if the penultimate chips were 25-35 mm apart, a single chip was removed half-way between them. Prior to sampling, the cross section was decontaminated by swabbing with tissue soaked in 70 percent ethanol. Conical sample chips were formed with two inclined cuts from a U-shaped gouge. The pointed end of the chip was pushed into a selective agar medium with the original decontaminated surface horizontal. This permits fungi from 3-5 mm below the original surface, unaffected by the 70 percent alcohol, to grow directly into the agar (see Figures 3 to 9). The agar medium (Morris, Dickinson and Levy, 1984) contains 2.0 percent malt extract, 3.0 mg Benomyl (selective for basidiomycetes) and 100 mg Streptomycin (selective against bacteria).

The samples were incubated at 25°C and examined after 0.5, 1, 2 and 4 weeks. The fungi isolated were subcultured and examined for the growth habit and presence of clamp connections which are diagnostic features of basidiomycetes. Isolates were identified by the initial letters of the wood species and a suffix "a" or "b" for different basidiomycetes from the same log.

Almost all the slices yielded isolates from large areas of the visibly decayed wood, which did not possess these diagnostic features. It was necessary to determine whether these were WRB, secondary non-wood rotting basidiomycetes or secondary non-wood rotting mould fungi. This could be done by identifying the fungi as known wood-rotting species or by assessing their decay capability directly. As this project was directed towards decay detection, it was felt that categorization of these isolates should be on functional criteria. A modification of the AWPA M-10 (American Wood Preservers' Assocation, 1986) soil block test was therefore used to assess their ability to cause weight loss in wood. The method was similar to that given in the M-10 standard with the exception of: (1) a reduced block size, 14 mm rather than 19 mm; (2) three blocks rather than two per soil jar; (3) an eight week rather than a twelve week incubation period; and (4) the use of the non-standard fungi under test.

Ponderosa pine sapwood was used for fungi isolated from softwoods and aspen sapwood was used for fungi isolated from Populus sp.

At the completion of this test the results for four of the isolates were found to be inconclusive. It was therefore necessary to attempt the identification of the isolates by comparison with known isolates from culture collection or by the use of selective enzyme reagents and microscopic features (Stalpers, 1978).

### 4.1.3 Moisture Content and Specific Gravity Determination

Blocks representing both sound and decayed wood were chosen from the discs used for decay assessment to determine both moisture content and specific gravity. The number of blocks per disc varied from 18 to 39. The green weight and oven dry weight were used for moisture content determination. The specific gravity was determined using the green volume and the oven dry

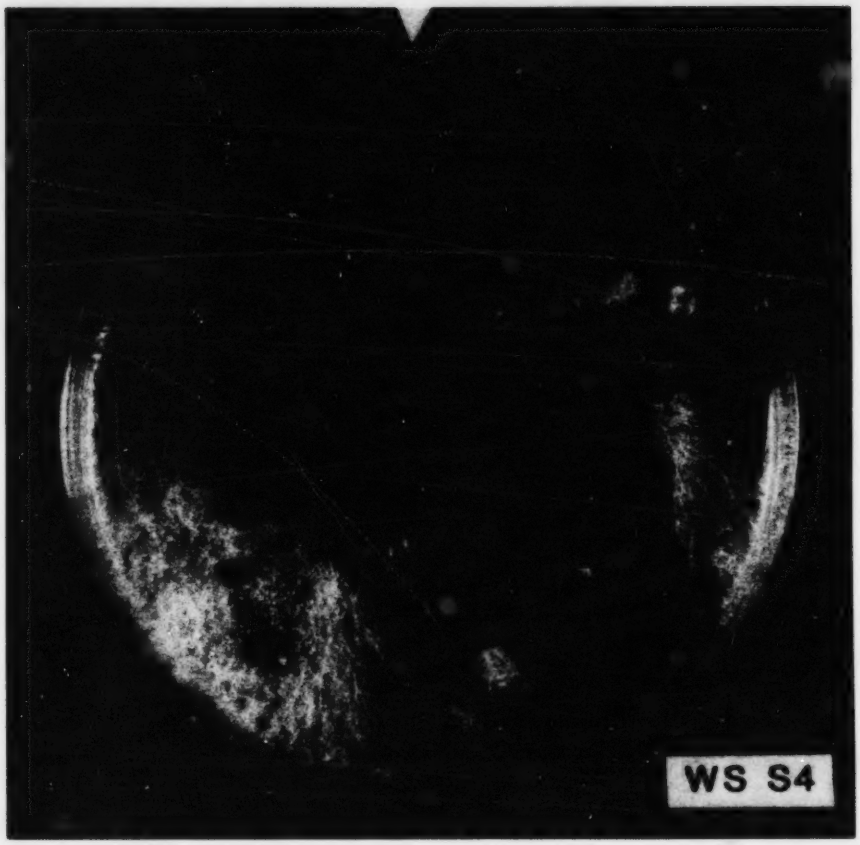


Figure 3. This agar plate was inoculated with five chips from the sapwood of white spruce. Two basidiomycetes have grown out: Isolate WSa, unidentified, from the chip at the top left and Isolate WSb, Armillarea sp., from the chip at the top of the plate.

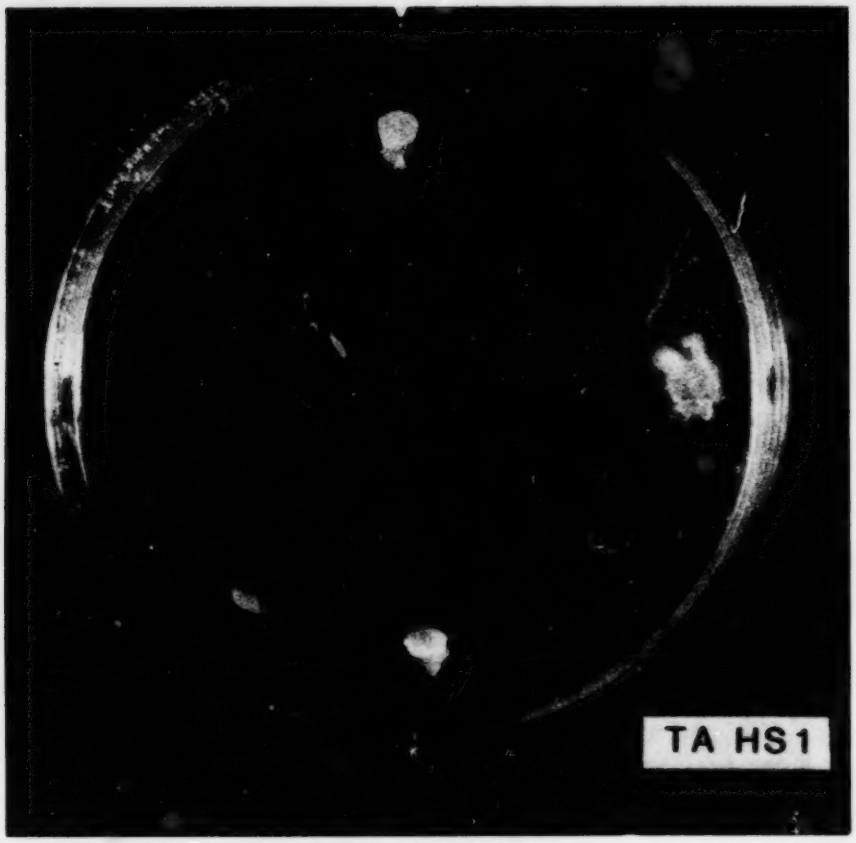


Figure 4. Five of these eight chips from the heartwood/sapwood boundary in trembling aspen have yielded Isolate TAa, a very slow growing fungus without the characteristic appearance of a wood rotting basidiomycetes: Phellinus tremulae.

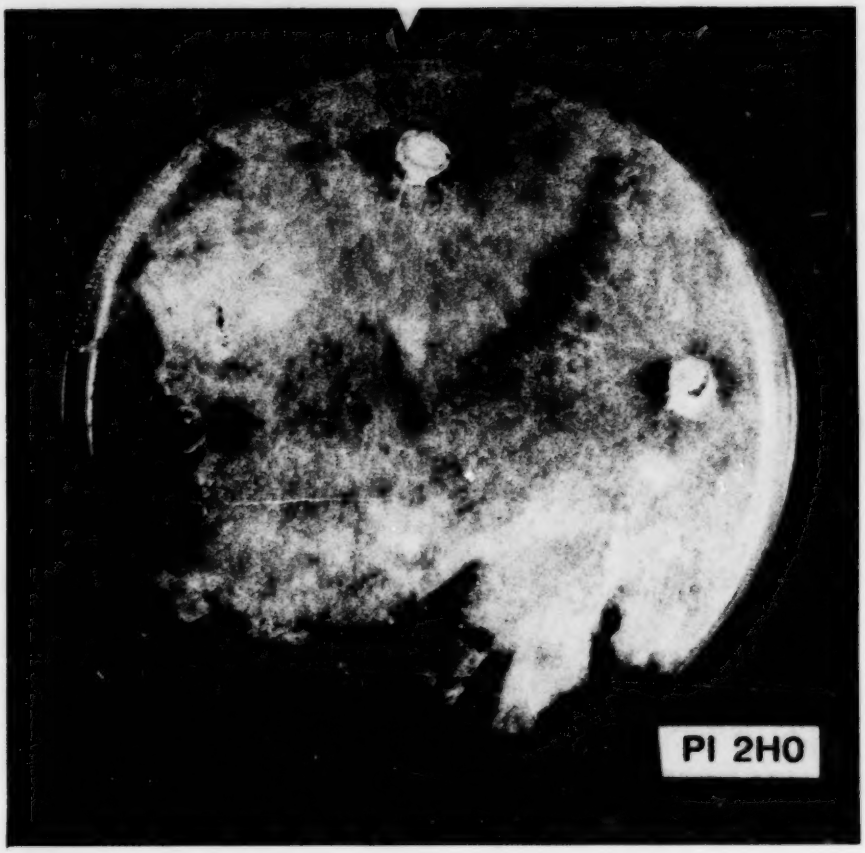


Figure 5. Two of these chips, top and left, taken from the second heartwood sampling annulus in lodgepole pine, have yielded Isolate LPa, a fungus of basidiomycete appearance which does not produce characteristic clamp connections: Phellinus pini.

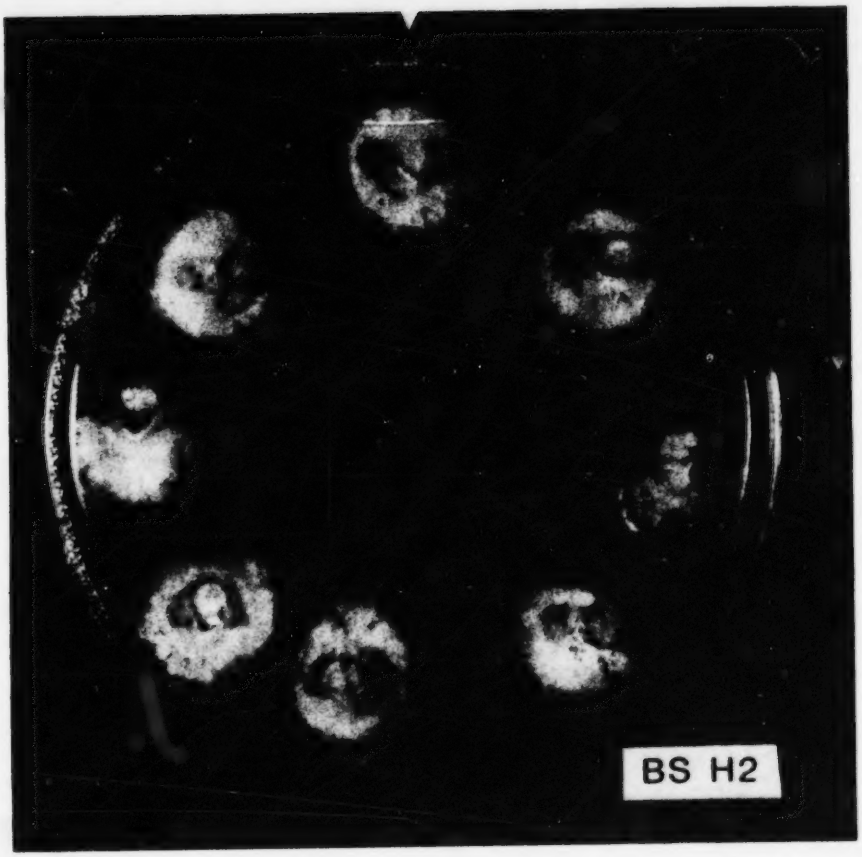


Figure 6. All eight of these chips from the heartwood of black spruce have yielded Isolate BSa, tentatively identified as Stereum sanguinolentum.

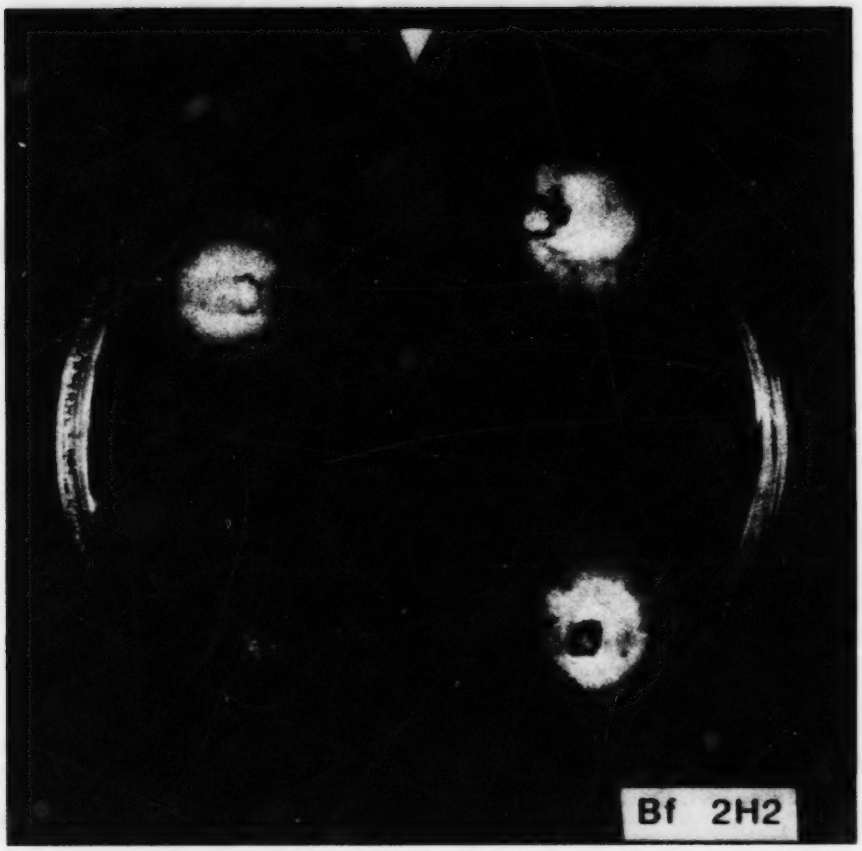


Figure 7. Three of these four chips from balsam fir heartwood have yielded Isolate BFa, Stereum sanguinolentum. The fourth chip has a non-basidiomycete fungus which was inhibited by the selective medium.

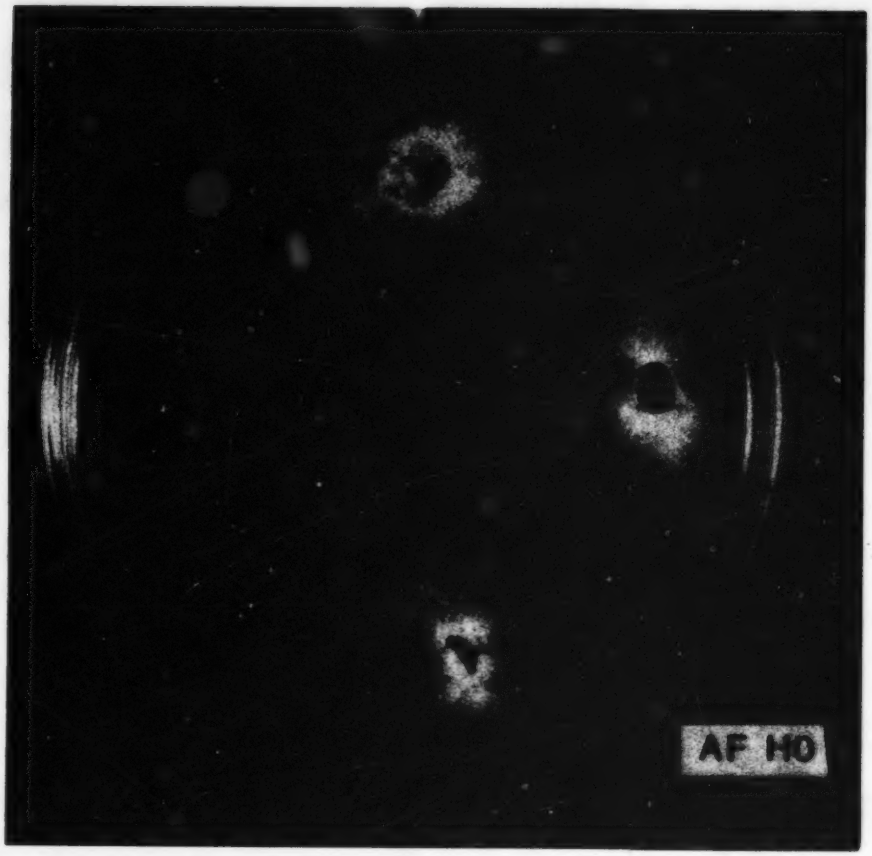


Figure 8. Three of these chips from alpine fir heartwood have yielded Isolate AFa, Stereum sanguinolentum. The fourth has a non-basidiomycete fungus which was inhibited by the selective medium.

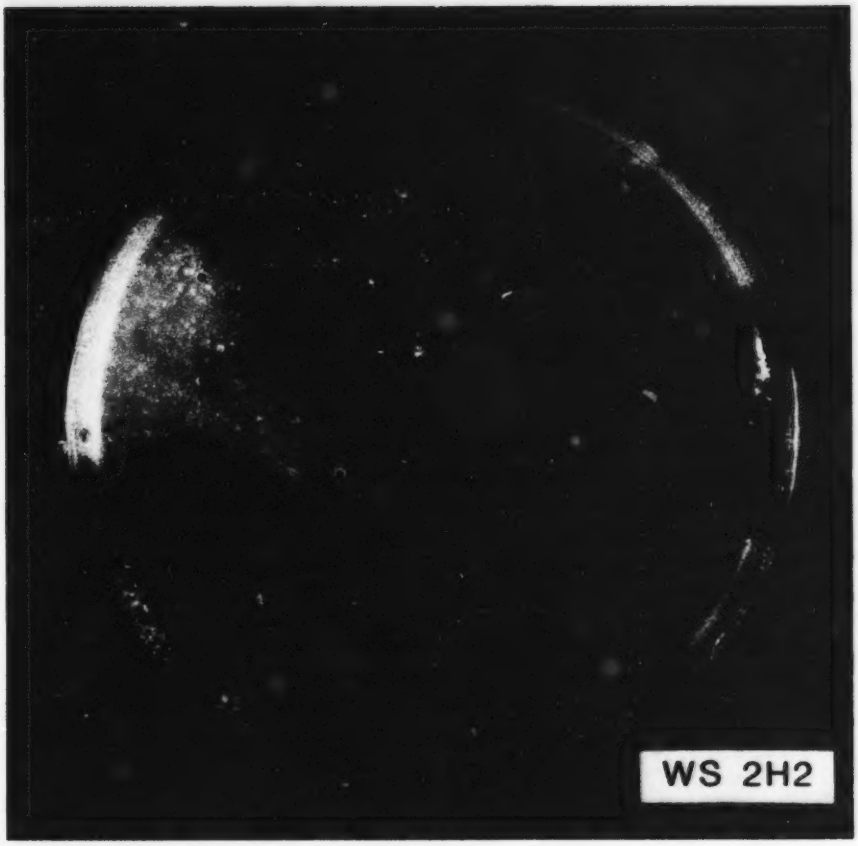


Figure 9. All seven of these chips from the heartwood of white spruce have yielded Isolate WSb, easily identified as an Armillerea by the black root-like mycelial cords, rhizomorphs, characteristic of this genus.

weight. The green volume was measured by saturating the samples in water by submerging the blocks in water and subjecting them to 1-1/2 hours of vacuum followed by 1-1/2 hours of pressure. The calculation of the specific gravity is then given by (Smith, 1954):

$$\text{specific gravity} = \frac{1}{\frac{M_S}{M_{OD}} - 0.346}$$

where $M_S$ = saturated weight; $M_{OD}$ = oven dry weight.

4.1.4 MR and CT Imaging

Magnetic resonance (MR) images were obtained from a single 10 mm slice, four inches from one end (Slice 1, four inches from decay assessment Slice 1A) of each of the seven species at the end of July, 1986. A Picker scanner with a 0.15 Tesla superconducting magnet, housed at the University of British Columbia (UBC), was used. A specially designed multiple echo protocol designated 51 ME6SS was developed to image as wide a range of echo values (TE) as possible (scans for each of the following TEs were obtained: 26, 52, 78, 104, 130 ad 156 millisec.). The following additional parameters were used: repeat time (TR) of 500 milliseconds; 8 repetitions; 256 views; a 30 cm field, and 17 min. scan time.

In addition, the trembling aspen segment (Slice 1) was scanned on the more powerful Philips Gyroscan 1.5 Tesla imaging system at the Montreal Neurological Institute (MNI) on August 20, 1986. A TR of 500 msec was used with 8 repetitions for a slice thickness of 10 mm. There were 8 multiple echo times imaged with TE = 30, 60, 90, 120, 150, 180, 210 and 240 msec. Three additional T2 images and three RH (proton density) images were produced using TE = 30 msec with 8 repetitions and the total signal from 8 echos.

Computed tomographic (CT) X-ray images were obtained for the same single slice (Slice 1) used for MR images for each of the seven species on July 31, 1986. An additional image was obtained four inches in from the opposite end of each log segment (Slice 2, 4 inches from decay assessment Slice 2A). A Siemens DR2 scanner housed at the University of British Columbia was used. The scan time was two seconds per each 8 mm slice using a 125 KV X-ray source giving a resolution of 1 mm.

Each image had "N", "S", "E" and "W" quadrants designated for ease of comparison with each other and for correlation with the previously described decay assessment.

4.1.5 Photographic Imaging

For visual comparison of the wood quality and decay present in each log segment with the corresponding MR and CT images, the center of the plane

through which the images were made was sawn open and a color and a black and white photograph taken.

## 4.2 RESULTS

The MR, CT and photographic images, fungi location figures and moisture content and specific gravity overlays are presented as Figures I-1 through I-119 in Appendix I. The order of the species is trembling aspen, balsam poplar, lodgepole pine, alpine fir, balsam fir, black spruce and white spruce. Within each species the order of the figures are: MR images, CT images, color photographs, black and white photographs, fungi location and moisture content and specific gravity overlays (e.g., I-28 and I-30). Refer to pages viii to xi for a detailed listing of the figures. For lodgepole pine and white spruce there were respectively only one and four MR images obtained for the short TE values because of low moisture content.

The distribution of wood rotting basidiomycetes (WRB) and of bacteria in the cross sections sampled (represented as coloured dots) is presented in Figures I-27, I-29 for trembling aspen; I-43, I-45 for balsam poplar; I-54, I-56 for lodgepole pine; I-70, I-72 for alpine fir; I-86, I-88 for balsam fir; I-102, I-104 for black spruce; and I-116, I-118 for white spruce.

Each sample position where microorganisms of interest were located has been colour coded for type of fungus or bacterium. Unlabelled positions were either sterile or yielded no fungi known to be associated with basidiomycete decay. Red spots represent WRB; green spots represent non-wood rotting fungi associated with decayed wood; and yellow spots represent bacteria possibly associated with decay or with wetwood.

## 4.3 DISCUSSION

### 4.3.1 Decay Assessment

#### Decay Capability of Isolates

Only two of the isolates tested, WSa (Figure 3) and BPa, from white spruce and balsam poplar, respectively, demonstrated an ability to cause rapid mass loss in the M-10 test (Table 2). Isolate TAa from trembling aspen caused a comparatively low weight loss, but this may be explained on the basis of its very slow growth rate. The results for the remaining four isolates were inconclusive. Weight losses caused by the isolates from alpine fir (AFa) and balsam fir (BFa) were less than the level (three percent) regarded as significant. The isolate from lodgepole pine (LPa) was borderline, while the isolate from black spruce (BSa) was barely significant.

#### Identification of Isolates

Isolate TAa (Figure 4) was identified as *Phellinus tremulae* (Bond) Bond and Borsov, using Stalpers' (1978) key to the Aphyllophorales. This fungus is by far the most common cause of heart rot in trembling aspen in Canada (Hepting, 1971), but has commonly been referred to as *Fomes ignarius* (L ex Fr) Kickx.

Table 2

Weight Loss and Identity for Wood-Rotting Basidiomycete Isolates

| Isolate Number | Identity if Known | Mean Percent Weight Loss | Wood |
|---|---|---|---|
| WSa | Unidentified | 20.57 | Pine |
| WSb | *Armillarea* sp. | NT | - |
| BSa | *Stereum sanguinlolentum* | 5.27 | Pine |
| BFa | " " | 1.98 | Pine |
| AFa | " " | 2.70 | Pine |
| LPa | *Phellinus pini* | 3.25 | Pine |
| BPa | Unidentified | 24.47 | Aspen |
| TAa | *Phellinus tremulae* | 9.01 | Aspen |
| Control | None | 0.56 | Pine |

NT - Not tested

The isolate from lodgepole pine (Figure 5), with a barely significant weight loss, was identified as Phellinus pini (Thore ex Fr.) Pilat, one of the most common causes of stain and heart rot in lodgepole pine in Alberta (Loman and Paul, 1963; Robinson-Jeffrey and Loman, 1963).

The isolates from black spruce (BSa), balsam fir (BFa) and alpine fir (AFa), with very low weight losses, were very similar to each other in appearance Figures 6, 7 and 8, respectively). On the basis of microscopic characteristics and comparison with culture collection strains these three were tentatively identified as Stereum sanguinolentum (Alb & Schw. ex Fr.) Fr. Isolate BSa differed from the other two in some microscopic features and in its capacity for decay. This fungus does not cause rapid weight loss in laboratory experiments (Ammer, 1963) as found in this study. It is, however, by far the most common for heart rot of balsam fir and alpine fir (Hepting, 1971). It is also one of the two most common heart rot fungi in black spruce, the other being Phellinus pini (Hepting, 1971). Both of these fungi rapidly colonize heartwood, causing a red stain. This is followed by a slow decay of the wood.

The most frequent isolate from the white spruce log, WSb, was easily identified as an Armillarea sp. by the presence of rhizomorphs in culture (Figure 9). Fungi of this genus are well known as causes of butt rot; consequently it was unnecessary to test its decay capability.

As a result of the decay testing and identification procedures, all the suspected basidiomycetes could be classified as WRB.

Location of Wood-Rotting Basidiomycetes

Trembling Aspen. Slices 1 and 2 (Figures I-27 and I-29): Phellinus tremulae was isolated from most of the sampling positions within the zone with visible evidence of decay. This WRB was present up to and just beyond the dark border of the damaged region; presumably a physiological reaction zone caused by the fungus or by the tree. Bacteria were isolated from a pocket of discoloured wet wood in Slice 2. The absence of the dark border at some points suggests that the fungus has broken through this barrier. The remains of a previously breached barrier can be seen towards the centre of the log.

Balsam Poplar. Slices 1 and 2 (Figures I-43 and I-45): The two single isolations of an unidentified WRB are probably of no significance, particularly as they are not in corresponding positions in the two slices and were not associated with any signs of decay. The patch of discoloured wood, at least in Slice 1, was associated with bacteria. These two slices both appear to be otherwise sound.

Lodgepole Pine. Slices 1 and 2 (Figures I-54 and I-56): The stain and heart rot fungus Phellinus pini was isolated from the whole of the area of discoloured wood in Slices 1 and 2 and from a few positions in visibly unchanged wood in Slice 2.

Alpine Fir. Slices 1 and 2 (Figures I-70 and I-72): The scarcity of isolations of Stereum sanguinolentum from Slice 1 compared to Slice 2 has no explanation at present. This fungus was found over the whole of the

discoloured area of Slice 2, even extending into protrusions of discolouration into the sapwood.

Balsam Fir. Slices 1 and 2 (Figures I-86 and I-87): In both slices Stereum sanguinolentum was isolated from the whole of the central discoloured zone and several points in the apparently sound sapwood.

Black Spruce. Slices 1 and 2 (Figures I-102 and I-104): The isolate tentatively identified as Stereum sanguinolentum was isolated from the whole of the discoloured zone in both slices up to the visible boundary but not beyond.

White Spruce. Slices 1 and 2 (Figures I-116 and I-118): Isolates of wood-rotting basidiomycetes representing two species were located from the whole of the visibly decayed zone in both slices. Isolate WS2, the Armillarea sp., accounted for the majority of these whereas the unidentified isolate WS1 was found in only a few sites in the sapwood. This log exhibited the most advanced decay including shrinkage and consequent voids.

Comparison of CT and MR Images with Fungal Isolations

Trembling Aspen. The X-ray CT scan (Figures I-21 and I-22) picked up distinct changes in density between decayed and undecayed heartwood in both slices, although measurements of specific gravity (Figures I-27 and I-29) did not pick up any recognizable differences. This may be partly due to a lower moisture content in the decayed wood in the centre of the log (Figures I-28 and I-30). Although this moisture content was above the minimum necessary for MR (about 40 percent), it did not show up to any great extent in the MR (Figures I-1 to I-6), suggesting a very rapid relaxation time, $T_2$. The MR images taken with the higher field strength (Figures I-7 to I-20) show more signal in the heartwood; however, a comparison of Figures I-7 through I-15 indicates a reduction in $T_2$. The band of wet wood at the edge of the decay pocket (Figure I-25), a well-known feature of decay by P. tremulae (Shigo, 1963) was detected by the CT and by the MR. They also detected the remains of an old decay boundary in the centre of the log.

A patch of bacterial wetwood discoloured grey in the colour photograph (Figure I-25) was also effectively imaged.

Balsam Poplar. The successful MR imaging of the sound heartwood of the balsam poplar (Figures I-31 to I-36), despite moisture contents as low as those found in the aspen, adds weight to the indication that the MR image is affected by decay. Unfortunately, in this preliminary study sound and decayed samples of each species were not available for direct comparison. There was still a small difference between the $T_2$ in the heartwood and the sapwood of balsam poplar. This may be due to the presence of extractives in the heartwood as well as the high moisture content and larger amount of unbound water in the sapwood (Figures I-31 to I-36). Both the CT (Figure I-37) and the MR (Figure I-31) picked up the area of bacterial wetwood, discoloured a rusty red in the photograph, and there were indications of a band of wet wood around the heartwood/sapwood boundary.

Lodgepole Pine. The CT (Figures I-48 and I-49) and MR (Figure I-47) both failed to distinguish the area of incipient decay in this log, possibly due entirely, in the case of the MR, and partly, in the case of the X-ray, to its low moisture content--near or below 40 percent. Even at generally higher moisture contents the CT would only be able to detect this very early stage of the decay process if there were some variation in moisture content caused by the fungus. Although no change in density has been recorded (and P. pini does not have a rapid rate of decay), there may clearly be some effect on strength and on pulping properties.

Alpine Fir and Balsam Fir. The scanning results for these two logs (Figures I-58 to I-65 and I-74 to I-81) were almost identical, as were the fungi isolated (Table x) and the patterns of decay observed (Figures I-70 and I-72, I-86 and I-88). The CT did not detect any difference in density between sound and discoloured timber (Figures I-64 and I-65, I-80 and I-81) but showed up the preponderance of wet pockets in the sapwood of both logs. The MR also picked up these wet pockets but did not show up the discoloured heartwood, again suggesting a possible effect of fungal activity on $T_2$.

Black Spruce. Moisture contents in the decayed heartwood (Figures I-103 and I-105) were somewhat marginal for MR imaging but the difference in decayed wood/sound wood contrast between the MR (Figures I-90 to I-95) and the CT (Figures I-96 and I-97) suggests some effect other than moisture content in the MR image. For example, a difference in the MR image between decayed heartwood and a small band of sound heartwood is particularly encouraging. Smaller moisture content samples would indicate if this difference was simply a moisture content difference, or, as suggested, an indication of the presence of decay.

White Spruce. This log, although meeting the requirement of being fresh cut, and having some decay present, was much too dry (Figure I-117) for MR imaging across most of the cross section (Figures I-106 to I-109). Only the wet boundaries of the decayed wood and small wet pockets were seen.

Due to the large density changes caused by the decay, the CT (Figures I-110 and I-111) produced an excellent image of the severely decayed timber. Some patches of early stages of decay (arrowed on Figures I-111 and I-114) were not so well-defined. This type of decay, a butt rot, often does not extend far up the trunk and proceeds directly through the decay process rather than rapidly staining and slowly damaging the timber like some of the fungi in other logs. It may therefore be particularly suitable for studying the detection of this type of butt rot at various stages.

### 4.3.2 Wood Quality Assessment

In addition to the ability to identify decay in its various forms, the CT and MR images allow evaluation of various additional wood quality features as they appeared in the samples examined. Table 1 indicates the wood characteristics present in some of the experimental log sections. The CT and MR scanned sections were cut open to allow a subjective evaluation of the ability of CT and MR to detect the various wood characteristics. It must be noted that the CT images show density variations - a combination of specific gravity and moisture content. The MR images show moisture content variations related to

the presence of water in the cell cavities. Water in the cell walls cannot be imaged by MR since the minimum TE possible with the UBC imaging scan sequence is 26 milliseconds. A TE of one to five milliseconds would allow the imaging of cell wall water. Since it is this water component that should be influenced the most by chemical environment, such as the effects of decay, imaging systems that can see this component need to be developed for large samples. The current ability of MR systems to see only the longer $T_2$ components does not preclude their use for decay detection, but further studies are required.

Sound Knots. Sound knots appear in the first slice of black spruce section (Figure I-98). The CT image (Figure I-96) shows the sound knot as an area of increased density. The MR image (Figure I-90) indicates the presence of the knot because of a moisture content reduction where the knot passes through the sapwood. There is also a faint increase in moisture content around the knot in the heartwood. The second slice of the lodgepole pine section (Figure I-52) shows five live knots. The CT image (Figure I-49) shows the knot presence by a similar increase in density. The two live knots in the second slice of the trembling aspen (Figure I-25) also are indicated in the CT image (Figure I-22) as an increase in density.

Dead Knots

Dead knots show up in the first slice of the balsam poplar sample (Figure I-39). The CT image (Figure I-37) shows the larger dead knot in the South position as an area of relatively uniform density. The second very small dead knot at the NW position shows up as an increased density area. A comparison of this area in the MR image (Figure I-31) shows up as an increase in moisture content, indicating the apparent density increase in the CT image results from an increase in moisture, not a specific gravity increase.

Unsound Knots. Unsound knots appear in the first slice of the alpine fir section (Figure I-66). The CT image (Figure I-64) indicates the presence of these knots as a density increase. Comparison with the MR image (Figure I-58) indicates that this is not only due to an increase in moisture content but also an apparent increase in extractive content. The unsound knots show up as moisture content increases in the heartwood and sapwood.

Compression Wood. Compression wood is present in the first slices of both the black and white spruce samples (Figures I-98 and I-112, respectively). The CT image (Figure I-96) for the black spruce shows the compression wood at the E position as an area of increased density; however, this is inconclusive. The black spruce MR image (Figure I-90) shows the compression wood as an increase in the moisture content as well as an increase in the annual ring width. This is slightly more conclusive. The white spruce CT image (Figure I110) again shows the compression wood at the NW position as an area of increased density. This image shows the compression wood more conclusively. The MR image (Figure I-106) gives no signal for most of the section due to moisture contents less than required for imaging of the water location, making evaluation of the compression wood impossible. The same conclusions may be drawn from the second slices of black and white spruce (Figures I-100 and I-114) when compared to the respective CT images (Figures I-97 and I-111).

Stain. The only sample showing stain (bluestain) is the lodgepole pine (Figures I-5- and I-52). The stain is in the sapwood and the CT images (Figures I-48 and I-49) show the sapwood as being an area of lower density. However, this is not conclusive to the identification of stain since there are areas in the sapwood with no apparent stain. The first slice (Figure I-47) has too low a moisture content to allow adequate imaging by MR of the stain area by this technique.

Checks and Splits. These characteristics are present only in the white spruce samples. Because the checks at the SSE position in the sapwood of the first slice (Figure I-110) are very small, the resolution of the CT image (Figure I-110) which is approximately 1 mm and the resolution of the MR image (Figure I-106) which is approximately 2 mm, would preclude their identification. The split at the N position, since it is quite wide, shows up in the CT image. Again, the low moisture content of the sample makes evaluation of the MR image for this characteristic impossible. The second slice of the white spruce (Figure I-114) has larger splits at the SE and SSW positions. These are readily seen in the comparable CT image (Figure I-111).

Pith. The location of the pith is quite visible in the CT images. It is also visible in the MR images for at least the shortest TE value (26 milliseconds) for all the species despite relatively low moisture contents in the heartwood of all but the balsam poplar samples. The first slice of the lodgepole pine (Figure I-50) with the lowest moisture content, even shows up a faint image of the pith in the comparable MR image (Figure I-47). All of the MR images of the balsam poplar (Figures I-31 to I-36) indicate the pith presence because of high moisture content (Figure I-44).

Juvenile Wood. There is juvenile wood in all of the species examined. The CT images of all but the white spruce samples (Figures I-110 and I-112) indicate clearly a decrease in density in the juvenile wood portion of the cross section. What appears to be the juvenile wood area shows up in the MR images for only the balsam poplar (Figures I-31 to I-36) and to a small degree in the trembling aspen (Figures I-1 to I-20), black spruce (Figure I-90) and the white spruce (Figure I-106). These latter three species show an increase in moisture content associated with the juvenile wood area, although this is not uniform within the whole of what appears to be juvenile wood area.

Sapwood/Heartwood Boundary. The sapwood/heartwood boundary is easily identified in both the CT and MR images of balsam poplar, trembling aspen, alpine and balsam fir and black spruce. For lodgepole pine and white spruce only the CT images indicate the boundary. The low moisture content of the sections of these two species precludes identification of the boundary from the MR images.

Extractives. Because of the presence of extractives in the heartwood the differentiation of the sapwood/heartwood boundary discussed previously gives rise to some information about the presence of extractives. Two species which give an indication of extractives being present are the MR images of the alpine and balsam fir (Figures I-58 to I-63 and I-74 to I-79). This observation is based on the rather high moisture contents present throughout the cross sections (Figures I-71; I-73; I-87 and I-89). These high moisture contents would normally be easily imaged by MR. The extractives and/or the

fungal activity discussed earlier would appear to have reduced the $T_2$ value of the water in the heartwood.

Specific Gravity. The specific gravity is shown in part by each of the CT images. There is, however, the confounding factor of the moisture content affecting the density value given by X-ray attenuation. Comparison of the MR with the corresponding CT image for each species would allow removal of variation caused by water in the cell cavities to give a clearer indication of specific gravity variation across the section. The water in the cell walls cannot be imaged by MR, so this component of the CT image cannot easily be adjusted.

Low Specific Gravity. Low specific gravity areas resulting from decay and apparent juvenile wood have been covered in previous sections.

Moisture Pockets. Moisture pockets are present in the balsam poplar, alpine and balsam fir and to a limited degree in white spruce. The pockets clearly show up in the MR images of the first slices (Figures I-31 to I-36; I-58 to I-63; I-74 to I-79; and I-106 and I-107). These pockets also show up in all of the CT images (Figures I-37 and I-38; I-64 and I-65; I-80 and I-81; and I-110 and I-111) as an increase in density. The moisture distribution in the alpine and balsam fir samples (Figures I-71 and I-73; I-87 and I-89) indicates many small pockets of moisture which relate to problems encountered in drying these species.

Wood Species. The separation of wood species by imaging can only be demonstrated from the MR images of the alpine and balsam fir samples (Figures I-58 to I-63 and I-74 to I-79). The apparent characteristic moisture distribution pattern was not present in any other species. The extremely high moisture content of the balsam poplar (Figures I-44 and I-46) may also be a characteristic allowing some species separation as shown in both the CT and MR images (Figures I-37 and I-38 and I-31 to I-36). The separation of species by specific gravity does not appear to be possible by either CT or MR and is certainly not apparent from the samples examined.

### 4.3.3 MR Imaging Using High Field Strength

The trembling aspen was imaged using both a 0.15 Tesla (UBC) and a 1.5 Tesla (MNI) magnet. The resolution of the growth rings was much greater for the higher field (Figures I-1 and I-7). The detail in the heartwood was greater with the higher strength magnet, particularly with the $T_2$ eight echo summation (Figures I-6 to I-18). The boundaries surrounding the decayed areas are also much clearer (Figures I-7 to I-20) for the high strength magnet than for the UBC system (Figures I-1 to I-6). Small changes in water distribution are more noticeable in the proton density map (Figures I-18 to I-20), than in the other images (Figures I-1 to I-17).

## 4.4 CONCLUSIONS

The MR and CT scans provided a PRELIMINARY evaluation of the ability of these techniques to detect the degree of decay and wood quality present in the sample log sections.

The samples examined provided a PRELIMINARY evaluation of two scanning techniques to detect internal characteristics. Magnetic resonance imaging requires moisture content in excess of the fibre saturation point. Many wood characteristics present in the sample logs were detectable using MR imaging. Decay was detected in trembling aspen, alpine and balsam fir and black and white spruce with a resulting apparent reduction in the spin-spin relaxation time ($T_2$). Sound knots were detected in black spruce; dead knots were detected in balsam poplar, and unsound knots were detected in alpine fir. Compression wood was partially identified in both black and white spruce. The pith is identifiable in all the species. Juvenile wood in balsam poplar, trembling aspen, black spruce and white spruce was detected to varying degrees. The sapwood/heartwood boundary is clearly shown for balsam poplar, trembling aspen, alpine and balsam fir and black spruce. The presence of extractives and/or fungal activity is indicated in alpine and balsam fir as a reduction in $T_2$ in the heartwood. Moisture pockets are detected in balsam poplar, alpine and balsam fir and white spruce. The characteristic MR images of alpine and balsam fir may allow separation of these species from others using this feature. The high moisture contents of the trembling aspen and the balsam poplar may allow separation of these species from others. The ability to identify similar defects in the species other than those listed above was not possible since the defects did not exist in all samples. Magnetic resonance imaging was unable to identify some defects because the moisture content was too low (less than 40 percent). It is expected, however, given sufficient moisture, that these defects in species such as lodgepole pine and white spruce can be detected by MR. The higher field strength of the MNI system gives improved resolution and additional signal in the heartwood of the trembling aspen sample.

Many wood characteristics present in the sample logs were detectable using X-ray CT imaging. Decay was detected in trembling aspen, black and white spruce. Sound knots were identified in trembling aspen, black spruce and lodgepole pine. Dead knots were detected in balsam poplar while unsound knots were detected in alpine fir. The identification of compression wood in black and white spruce was inconclusive. Splits and checks were identifiable in white spruce. The pith was easily identified in all species. Juvenile wood of all but white spruce was identified as an area of lower density. The sapwood/heartwood boundary was identifiable for all species. Moisture pockets are detected in balsam poplar, alpine and balsam fir and white spruce. Separation of balsam poplar, due to its very high moisture content, may allow separation of this species from others. Computed tomography can image at any moisture content; however, the information is limited to the relative density changes which are a combination of specific gravity and moisture content. In addition, X-rays have a low tolerance to wide variations in density, making some characteristics difficult to identify.

Incipient decay in lodgepole pine was not detectable by either imaging system possibly due to its low moisture content. Blue stain, also present in the lodgepole pine, was similarly not detectable. Further work is necessary, particularly with imaging of the cell wall water component, to determine the ability of MR to identify these defects.

# 5.0 APPLICATION OF SCANNING AND IMAGING TO PRIMARY MILLS AND FORESTS

## 5.1 PRIMARY MILLS

The internal scanning of logs for decay and wood quality must lead to an increase in product value to justify a major capital expenditure for such equipment. For softwoods of large diameter, where grade recovery is to be maximized, knowledge of the internal characteristics can be used to derive the sawing solution.

However, the determination of the magnitude of potential increases in value or volume recovery due to technology that will detect and identify internal defects is not an easy task. The underlying assumptions about current practices and the potential improvement from the new technology must be carefully considered. The use of sawing simulation programs can shed some light on the topic. Some estimates of improved recovery from the worst to the best log rotation range from five to 22 percent (Wagner and Taylor, 1985). This does not completely addresss the real question about the effect of the internal characteristic on the achievable recovery or the current ability of the operator to make correct judgements. The work by the Japanese (Noguchi, 1985; Tochigi et al., 1983), which looks at the computer simulation of grain patterns on sawn surfaces, does address the question. Here, the differences in value recovery between the best sawing method and the worst was 20 percent. The conclusion they reached, however, was that the sawyer using human judgement did an equivalent job to the computer. If processing speed were increased or if the operator's skill decreased, then the computerized system would provide an improvement. In Sweden, the use of the TINA scanning system (Westergaard, 1986; Nystrom, 1985) has been driven by a 4:1 price difference between the highest grade pine and the fourth grade. Here, small improvements in grade outturn have a large effect on mill profitability. Studies are being proposed to develop extensive data bases (Wagner and Taylor, 1985; Johansson, 1985) to determine the potential benefits from internal log scanning.

The Instrument Development Branch of Atomic Energy of Canada Ltd. is concerned about the same questions. A confidential report by Woodbridge Reed and Associates (Division of H.A. Simons) done for them focussed on the target market, the potential degree of market penetration, and the forest resource and lumber marketing trends that could have an impact on the need for CT internal scanning. A separate determination of the potential improvements is required for each specific mill, since equipment, products, manpower, resource and markets are different.

An increase in value recovery of 10 percent represents about $4 MM per year for a mill producing 100 MM fbm per year for grade recovery (assuming an average price of $400 per Mfbm). For a similar small log sawmill producing 100 MM fbm of dimension lumber, an increase of five percent in value recovery represents additional revenue of $1.2 MM per year (assuming an average price of $240 per Mfbm). These types of increases in revenue are significant and appear to be a realistic expectation and could justify a reasonable expenditure to achieve them.

The cost of internal scanning technology has been estimated as high as $2 million for a medical type MR scanner down to about $0.6 million for a TINA type scanner. If increased revenues are in the range of five to 10 percent, then scanner systems with a cost of $0.5 to $1 million are not out of line. Because the degree of sophistication of most medical type scanners is high, technology must progress towards lower cost equipment, with sufficient resolution and speed for the purpose, before scanning systems such as these will be implemented in the forest industry. The current form of medical scanners with their circular gantry opening may be altered to provide better access. It is also necessary to have adequate computer programs to optimize the sawing patterns based on internal log defect information. Although these technologies are not ready for mill use yet, there are signs that some soon will be. For example, an X-ray system to scan logs for rot, knots and rocks may reach a prototype stage as soon as 1988 (Sorensen, 1986). Magnetic resonance systems that determine some of the wood characteristics of interest are possible within four to five years.

The primary industry in Alberta may look to the future use of internal scanning technology for use in the sawmills where optimum sawing patterns will ensure maximum value recovery. The use of the same technology in the plywood industry is also a likely possibility. For reconstituted panel product plants, a scanner for internal log quality may assist in making best use of the available raw material; higher quality wood can be diverted to more valuable uses. Any part of the manufacturing sector that is aiming at value added products may also be able to take advantage of such equipment to maximize value recovery. The available future technology may either be CT or MR, or perhaps a combination of the two. The preliminary demonstrated ability of MR to look at more than just nominal density variations will help to drive the continued development of this technology for application in primary plants. The CT imaging field is progressing and, as noted above, should see an industrially applied scanner for logs in about two years.

It should be noted that developments in both the microwave and ultrasonic fields may eventually lead to internal scanning systems capable of detecting internal characteristics with good resolution and defect identification for logs.

## 5.2 FOREST APPLICATIONS OF INTERNAL SCANNING

The benefits of internal scanning and imaging in the forests could have a potential impact on plant physiology, environmental assessment, silviculture, mensuration and harvesting. Since these techniques are non-destructive, the trees can continue growth without problems associated with other more destructive techniques which can range from cutting the tree down to removal of an increment core. The detection of decay is of prime concern, particularly decay which does not have external indicators. These techniques could also determine which trees are not worth harvesting before felling. The identification of incipient decay could aid in the prevention of its spread. The use of such technology to evaluate growth rates will help identify plus trees and the effects of silvicultural treatments. Studies on the physiology of living trees using MR techniques may also lead to enhanced growth. Techniques using CT (Habermehl, 1982a and b; Onoe et al., 1983; Onoe, 1986; Fox, 1983) can currently provide some of this information. The techniques

need to be refined for greater ease of application. Use of ultrasonics holds promise as a simpler and less costly technique, at least for rot detection in logs or standing timber. The MR technique needs to be further developed with the possible use of a lower magnetic field and a degree of portability not currently present.

The cost effectiveness of internal scanning and imaging in the forests depends on the potential benefit to the user which are related to the application. Defining the dollar value of the benefits is not easy. An increase in growth or increase in log grade due to a specific treatment can provide an estimate of value increase that can offset the scanning costs, including those of the scanner itself. If it is silvicultural techniques or treatments that are being evaluated, then the results should apply to large forested tracts, making an expensive scanner cost effective. If every tree needs to be scanned, then the cost and portability are an important concern.

The continued development of MR, CT and even ultrasonics should lead to portable scanning or imaging systems with suitable resolution of wood characteristics.

## 6.0 RECOMMENDATIONS FOR FUTURE RESEARCH AND DEVELOPMENT

Scanning techniques based on X-rays or ultrasonics rely on gross physical changes in wood properties. They have difficulty in locating the early stages of decay, which may still have significant effects on the wood quality, compression wood, stain and wood species characteristics such as extractives. Magnetic resonance scanning, which may detect changes at a molecular level, is therefore a more promising tool.

There are two directions which future research using MR should take. The first is an MR spectroscopic analysis of the following wood characteristics:

1. Clear, sound wood of all species. This will allow the characterization of sapwood, heartwood and juvenile wood as well as the effect of extractives on the MR signals.

2. Decayed wood of all species. This should investigate the effects of the presence of white and brown rot fungi and stain or mould fungi on MR. It should also incorporate evaluation of physical changes in the wood structure and the production of metabolites, particularly those with free radicals and the intermediates in lignin and cellulose breakdown.

3. Compression wood, tension wood, knots, stain, pitch pockets and moisture pockets.

The spectroscopic equipment necessary for such studies is outlined by Sternin (1985).

The second research direction is further MR imaging studies (coupled with comparative CT imaging). Field echo imaging should be explored which allows $T_2$ images to be produced with a TE of 13 to 18 milliseconds as compared to the 26 milliseconds of the current study. This technique, available on the UBC MR scanner, would allow more of the water to be successfully imaged. Fast imaging should be explored on both a 0.15 Tesla scanner (UBC), and with a high field strength 1.5 Tesla (Montreal Neurological Institute) scanner when the software to carry out the technique has been installed. There also exists a 1.5 Tesla scanner in Edmonton which should eventually have fast imaging software available. An imaging study must also be done with a scanner using a lower magnetic field coupled with fast imaging. The imaging of cell wall water (1 to 5 milliseconds) should provide additional correlation of decay and wood quality with MR parameters. This will require development of scanners able to do this.

The spectroscopic studies will allow a clear definition of the MR parameters ($T_1$, $T_2$ and proton density) so images can be correctly interpreted. The imaging studies will identify technologies which will speed up the collection and interpretation of the data.

Future developments for internal scanning of logs need to be aimed at the creation of a lower cost MR scanning system presumably using lower magnetic

fields with fast scanning. A computer program must be developed which takes advantage of the internal scanning data to optimize the processing system (i.e., log bucking, primary breakdown, remanufacture, veneer peeling, etc.). It would appear that such a program has been confidentially developed by M & B Research for their internal use.

The research outlined above has the potential to be accomplished in Alberta. The University of Calgary (M.R. Smith), Department of Electrical Engineering, has MR experience. A Phillips 1.5 Tesla MR imaging system is in use at the hospital facility in Edmonton. The Alberta Research Council has demonstrated software development expertise as shown by their program METEOR. The major forest products equipment companies are located in British Columbia; however, high technology equipment development should be able to take place in Alberta given the province's industrial capabilities.

## 7.0 REFERENCES

Allan, C.J.; Keller, N.A.; Lupton, L.R.; Taylor, T.; Tonner, P.D. 1984. Tomography - an overview of the AECL program. Atomic Energy of Canada Ltd. Report No.8571. 31p.

American Wood Preservers' Association. 1986. M10-77 Standard method of testing wood preservatives by laboratory soil block cultures. IN: American Wood Preservers' Association Standards, 1986.

Ammer, U. 1963. Studies on the growth of red stripe fungi in relation to wood moisture. Sanderdruck aus Forstw. Centralblatt 82(11,12):360-392.

Anon. 1981. A simple non-destructive means of testing poles in situ. Distribution, December, 1981:21.

Anon. 1983. PURL ultrasonic wood pole rot detector. Manufacturers Brochure, Biccotest Limited, Hertfordshire, England. 8p.

Anon. 1984a. No common steel nails allowed. Engineering News Record, December, 1984:36A.

Anon. 1984b. Scanning technology for the eighties. Seminar Proceedings, Forintek Canada Corp., Special Publication No.21:135.

Anon. 1985. Providing homes for high-priced imagers. High Technology, March, 1985:83.

Anon. 1986a. Book of Abstracts, Volume 1, Fifth Annual Meeting, Society of Magnetic Resonance in Medicine, August 19, 1986, Montreal, Quebec. 272p.

Anon. 1986b. Book of Abstracts, Volume 2, Fifth Annual Meeting, Society of Magnetic Resonance in Medicine, August 20, 1986, Montreal, Quebec. p.273-584.

Anon. 1986c. Book of Abstracts, Volume 3, Fifth Annual Meeting, Society of Magnetic Resonance in Medicine, August 21, 1986, Montreal, Quebec. p.585-1094.

Anon. 1986d. Book of Abstracts, Volume 4, Fifth Annual Meeting, Society of Magnetic Resonance in Medicine, August 22, 1986, Montreal, Quebec. p.1095-1584.

Anon. 1986e. Works in Progress, Fifth Annual Meeting, Society of Magnetic Resonance in Medicine, August 19-22, 1986, Montreal, Quebec. 282p.

Arita, K.; Mitsutani, S.; Sakai, H.; Tomikawa, Y. 1986. Detection of decay in the interior of a wood post by the ultrasonic method. Mokuzai Kogyo 41(8):370-375.

Aronson, R.B. 1984. A new way to see inside the body. Machine Design, June, 1984:25-28.

REFERENCES, Contd.

Asplund, T.; Johansson, L.G. 1984. Feasibility study of X-ray computerized tomography in research and development for wood-mechanical industry and forestry (in Swedish). Svenska Traforskningsinstitutet, Wood Technology Report No.53. 35p.

Ball, J; Simmons, G. 1984. Detection of bronze birch borers larvae and pupae by radiographs (Coleoptera:Buprestidae). The Great Lakes Entomologist 17(4):223-224.

Beaton, J.; White, W.B.; Berry, F.H. 1972. Radiography of trees and wood products. Material Evaluation, October, 1972:16A-17A.

Benson-Cooper, D.M.; Knowles, R.L.; Thompson, F.J.; Cown, D.J. 1982. Computed tomographic scanning for the detection of defects within logs. Forest Research Institute Bulletin No.8, New Zealand Forest Service, Rotorua. 9p.

Bergh, K. 1985. Fundamentals in microwaves. Proceedings of Internal Defect Scanning of Logs, Oslo, Norway, June 20-21, 1985. p.47-61.

Birring, A.S.; Smith, A. 1985. Radiographic and tomographic approaches to detect and measure deterioration in wood. Proceedings of 15th Non-destructive Symposium, San Antonio, Texas, April, 1985. 4p.

Birtz, R.E. 1984. Inspection of wood poles in place. Proceedings of Canadian Wood Preservers' Association, Toronto, Ontario, November 13, 1984. 7p.

Brownstein, K.R. 1980. Diffusion as an explanation of observed NMR behavior of water absorbed on wood. J. Mag. Reson. 40:505-510.

Burgess, A.E. 1985. Potential application of medical imaging techniques to wood products. Proceedings of 1st International Conference on Scanning Technology in Sawmilling, San Francisco, California, October 8-11, 1985. p.VII-1/VII-13.

Burgham, P. 1983. McDonnell Aircraft automates ultrasonic inspection. Manuf. Eng. 91(5):47-48.

Byrne, G.F.; Fenn, M.D.; Burgar, M.I. 1986. Nuclear magnetic resonance studies of water in tree sections. Agricultural and Forest Meterology. In Press. 11p.

Eslyn, W.E. 1968. Utility pole decay. Part I: appraisal of a device for non-destructive detection of decay. Wood Sci. Technol. 2:128-137.

Fox, B. 1983. Intensive care for trees. PIM 17(3):725.

Fullerton, G.D. 1982. Basic concepts for nuclear magnetic resonance imaging. Mag. Res. Imaging 1:39-55.

REFERENCES, Contd.

Funt, B.C.; Bryant, E.C. 1984. Towards automatic sawlog defect detection using computer tomography. Proceedings of Scanning Technology for the Eighties, Forintek Canada Corp., Special Publication No.21:16-20.

Gardner, W.D.; Johnstone, R.S.; Pitt, W. 1980. Detection of defects in standing poles by X-ray techniques. Document IRG/WP/2132, 11th Annual Meeting of the International Research Group on Wood Preservatives, Raleigh, North Carolina, May 5-9, 1980. 12p.

Goodell, B.S.; Graham, R.D. 1983. A survey of methods used to detect and control fungal decay of wood poles in service. International J. Wood Preservation 3(2):61-63.

Gosch, J. 1986. Speeding up NMR imaging to watch a kidney work. Electronics 59(6):19-20.

Graham, R.D.; Helsing, G.G. 1979. Wood pole maintenance manual: inspection and supplemental treatment of Douglas-fir and western red cedar poles. Forest Research Laboratory, Oregon State University, Corvallis, Research Bulletin No.24. 64p.

Gummerson, R.J.; Hall, C.; Hoff, W.D.; Hawkes, R.; Holland, G.N.; Moore, W.S. 1979. Unsaturated water flow within porous materials observed by NMR imaging. Nature 281(6):56-57.

Habermehl, A. 1982a. A new non-destructive method for determining internal wood condition and decay in living trees. Part I - principles, method and apparatus. Arboricultural J. 6:1-8.

Habermehl, A. 1982b. A new non-destructive method for determining internal wood condition and decay in living trees. II: results and further developments. Arboricultural J. 6:121-130.

Hailey, J.R.T.; Menon, R.S.; MacKay, A.; Burgess, A.E.; Swanson, J.S. 1985. Nuclear magnetic resonance scanning for wood characterization. Proceedings of 5th Symposium on Non-destructive Testing of Wood, Pullman, Washington, September 9-11, 1985. 17p.

Hall, L.D.; Rajanayagam, V.; Stewart, W.A.; Steiner, P.R. 1986. Magnetic resonance imaging of wood. Can. J. For. Res. 16(2):423-426.

Hall, L.D.; Rajanayagam, V. 1986. Evaluation of the distribution of water in wood by use of three dimensional proton NMR volume imaging. Wood Sci. Technol. In Press.

Harbich, W. 1984. Requirements and methods for the microcomputer-aided radiography of beech sawn timber (in German). Holztechnologie 25(4):189-191.

Hartley, P. 1986. Tomography - a sub-atomic look at engines. Engineering Digest. August, 1986. p.23-24.

REFERENCES, Contd.

Hattori, N.; Matsuyama, M.; Yamaoka, N.; Nishimura, K. 1985. Observation of the Japanese conifers by a medical X-ray computed tomography scanner. Proceedings of Internal Defect Scanning of Logs, Oslo, Norway, June 20-21, 1985. p.97-111.

Hattori, Y.; Kanagawa, Y. 1985. Non-destructive measurement of moisture distribution in wood with a medical X-ray CT scanner. I - accuracy and influencing factors. Mokuzai Gakkaishi 31(12):974-982.

Hattori, Y.; Kanagawa, Y. 1985. Non-destructive measurement of moisture distribution in wood with a medical X-ray CT scanner. II - changes in moisture distribution with drying. Mokuzai Gakkaishi 31(12):983-989.

Hepting. 1971. Diseases of forest and shade trees of the United States, U.S. Department of Agriculture, Forest Service Agriculture Handbook No.386. 658p.

Holland, J.F.; Heath, C.A. 1983. Sonic testing - a proven method through the use of electronic frequencies to determine the presence of decay in wood poles. Manufacturers Brochure, Heath Energy System, Richmond, Michigan. 12p.

Hsi, E.; Hossfield, R.; Bryant, R.G. 1977. Nuclear magnetic resonance relaxation study of water absorbed on milled Northern white cedar. J. Colloid Interface Sci. 62:389-395.

Jensen, L.C. 1965. Sonic detection of internal decay in wood poles. Proceedings of 2nd Symposium on Non-destructive Testing of Wood, Spokane, Washington, April, 1965. p.207-222.

Juvonen, R. 1985. Automatic lumber quality grading in practice. Proceedings of 1st International Conference on Scanning Technology in Sawmilling, San Francisco, California, October 8-11, 1985. p.XV-1/XV-5.

King, R.; James, W.L.; Yen, Y. 1985. A microwave method for measuring moisture content, density and grain angle of wood. Proceedings of 1st International Conference on Scanning Technology in Sawmilling, San Francisco, California, October 8-11, 1985. p.XVI-1/XVI-9.

Kogure, J.; Kawamura, H. 1984. Rot detection of wood poles for power distribution by means of a portable X-ray computed tomographic scanner. Japan IERE Council Special Document R-8401. 18p.

Kristiansen, U. 1985. Acoustics and defect location in wood. Proceedings of Internal Defect Scanning of Logs, Oslo, Norway, June 20-21, 1985. p.36-46.

Kucera, L.J.; Brunner, P.; Boesch, C. 1986. MR-tomography for our forests. Brooker Report 1(1):30-32.

REFERENCES, Contd.

Lee, I.D.G. 1958. Non-destructive testing of wood by vibration methods. Lecture to the Institute of Wood Science, November 12, 1958. 12p.

Liu, Z.; Dai, C.; Han, G. 1984. The nondestructive detection of defects in wood by X-ray transmissive technique. Sci. Silv. Sin. 20(2):220-223.

Loman, A.S.; Paul, G.P. 1983. Decay of lodgepole pine in two foothills sections of the boreal forest of Alberta. Forest Chron. 39:422-435.

MacGregor, R.P.; Peemoeller, H.; Schneider, M.H.; Sharp, A.R. 1983. Anisotropic diffusion of water in wood. J. Appl. Polym. Sci: Appl. Poly. Symposium 37:901-909.

MacKay, A.L.; Bloom, M.; Tepfer, M.; Taylor, I.E.P. 1982. Broadline proton magnetic resonance study of cellulose, pectin and bean cell walls. Biopolymers 21:1521-1534.

Magnusson, H.; Eriksson, L.; Andersson, L.D. 1972. Measurement of moisture content in wood and pulp samples using the NMR technique. Sven. Papperstidn. 75(15):619-622.

Mayer, D. 1985. Internal scanning for defect detection. An application of high technology in the operation of our forests and in the lumber manufacturing industry. Forintek Canada Corp., Vancouver, B.C., Technical Report 40-43-422. 31p.

Menon, R.S.; MacKay, A.L.; Hailey, J.R.T.; Bloom, M.; Burgess, A.E.; Swanson, J.S. 1987. An NMR determination of the physiological water distribution in wood during drying. J. Appl. Polym. Sci. In Press. 15p.

Miller, B.D.; Taylor, F.L.; Popeck, R.A. 1965. A sonic method for detecting decay in wood poles. Proceeding of the American Wood Preservers Association 61:109-115.

Morris, P.I. 1986. Forintek Canada Corp., Personal Communication.

Morris, P.I.; Dickinson, D.J.; Levy, J.F. 1984. The nature and control of decay in creosoted electricity poles. Rec. 1984 A Conv. Brit. Wood Preserv. Assoc. p42-55.

Morris, P.I.; Friis-Hansen. 1984. Report on a field demonstration of methods for detecting defects in wood poles. Document IRG/WP/2232, IRG Secretariat, Stockholm, Sweden. 4p.

Morris, P.I.; Waite, A.M.; Dickinson, D.J. 1984. The effect of moisture content on the electrical resistance of timber as detected by a pulsed current assistance meter (Shigometer). Intern. Res. Gp. on Wood Preserv. Doc. No. IRG/WP/2212. 11p.

REFERENCES, Contd.

Mothershead, J.S.; Stacey, S.S. 1965. Applicability of radiography to inspection of wood products. Proceedings of 2nd Symposium on Non-destructive Testing of Wood, Spokane, Washington, April, 1965. p.307-336.

Nanassy, A.J. 1973. Use of wide-line NMR for measurement of moisture content ion wood. Wood Sci. 5(3):187-193.

Nanassy, A.J. 1974. Water sorption in green and remoistened wood studied by the broad-line component of the wide-line NMR. Wood Sci. 7(1):61-68.

Nanassy, A.J. 1976. True dry-mass and moisture content of wood by NMR. Wood Sci. 9(2):104-109.

Nanassy, A.J. 1978. Temperature dependence of NMR measurement on moisture in wood. Wood Sci. 11(2):86-90.

Noguchi, M. 1985. Present state of computed sawing technique in Japan. Proceedings of Internal Defect Scanning of Logs, Oslo, Norway, June 20-21, 1985. p.10-23.

Nystrom, G. 1985. A system for measuring dimensions and quality of logs. Proceedings of Internal Defect Scanning of Logs, Oslo, Norway, June 20-21, 1985. p.5-9.

Ollson, M; Johansson, L.G.; Persson, B. 1985. Proton NMR measurements on wood. Proceedings of Internal Defect Scanning of Logs, Oslo, Norway, June 20-21, 1985. p.81-85.

Onoe, M. 1986. How to observe tree-rings without really cutting. Proceedings of International Symposium on Ecological Aspects of Tree-ring Analysis, Palisades, New York, August 17-21, 1986. 5p.

Onoe, M.; Tsao, J.W.; Yamada, H.; Nakamura, H.; Kogure, J.; Kawamura, H.; Yoshimatsu, H. 1983. Computed tomography for measuring annual rings of a live tree. Proceedings of Institute of Electrical and Electronics Engineers 71(7):907-908.

Parker, R. 1985. Restricted diffusion. Technical Presentation, Weyerhaeuser Technical Centre, Tacoma, Washington, May, 1985.

Parrott, R.E. 1965(?). Sonic detector picks decay. Timber Development Association (NZ) 2(4):3-4.

Peemoeller, H.; Hale, M.E.; Schneider, M.H.; Sharp, A.R. 1985. Study of restricted diffusion in wood. Wood and Fiber Sci. 17(1):110-116.

Pellerin, R.F.; De Groot, R.C.; Esenther, G.R. 1986. Non-destructive stress wave measurement of decay and termite attack in experimental wood units. Document IRG/WP/2256, 17th Annual Meeting of the International Research Group on Wood Preservatives, Avignon, France, May 26-30, 1986. 31p.

REFERENCES, Contd.

Portugal, F.H. 1984. NMR - promises to keep. High Technology, August, 1984:66-74.

Pykett, I.L.; Newhouse, J.H.; Buonanno, F.S.; Brady, T.J.; Goldman, M.R.; Kistler, J.P.; Pohost, G.M. 1982. Principles of nuclear magnetic resonance imaging. Radiology 143:157-168.

Riggin, M.T.; Sharp, A.R.; Kaiser, R.; Schneider, M.H. 1979. Transverse NMR relaxation of water in wood. J. Appl. Polym. Sci. 23:3147-3154.

Robinson-Jeffrey, R.; Loman, A.A. 1963. Fungi isolated in culture from red heartwood stain and advanced decay of lodgepole pine in Alberta. Can. J. Bot. 40:609-614.

Schmidt, T. 1978. Scanning/computing methods for measuring knots and other defects in lumber and veneers. Proceedings of 4th Non-destructive Testing of Wood Symposium, Vancouver, Washington. p.23-25.

Shigo, A.L. 1963. Fungi associated with discolorations around rot columns caused by Fomes ignarius. U.S. Dept. Agr. Plant Dis. Rep. No.47. p.820-823.

Singh, A; Jolly, W.D.; Krzywosz, K.J.; Kenny, C.A. 1983. Investigation of inspection techniques for timber waterfront structures. Proceedings of 13th NDE Symposium, San Antonio, Texas, April, 1983.

Smith, D.M. 1954. Maximum moisture content method for determining specific gravity of small wood samples. Forest Products Laboratory, Madison, Wisconsin, Report No. 2014. 8p.

Smith, R.S. 1984. Decay detection in situ. Proceedings of 5th Annual Meeting of Canadian Wood Preservers' Association, Toronto, Ontario, November 13, 1985. 16p.

Solberg, K.O. 1985. Determination of wood quality using nuclear techniques. Proceedings of Internal Defect Scanning of Logs, Oslo, Norway, June 20-21, 1985. p.62-72.

Sorensen, J. 1986. B.C. firms looking for ways to save downtime caused by rocks in wood. Logging and Sawmilling J., November, 1986:17-19.

Stalpers, J.A. 1978. Identification of wood inhabiting Aphyllophorales in pure culture. Studies in Mycology, No.16, Centraalbureau voor Shimmelcultures Barn. 248p.

Sternin, E. 1985. Data acquisition and processing: a systems approach. Rev. Sci. Instrum. 56(11):2043-2049.

Stott, M.A. 1969. Wood pole rot detection - an assessment of new and traditional approaches. Electrical Council Research Center, CITY, England. Report R-181. 20p.

**REFERENCES, Contd.**

Szymani, R. 1979. Defect detection systems for lumber: current status, trends and potential applications. Oregon State University Report, July, 1979. 70p.

Szymani, R. 1985. An overview of scanning technology in sawmilling. Proceedings of 1st International Conference on Scanning Technology in Sawmilling, San Francisco, California, October 10-11, 1985. p.I-1/I-33.

Szymani, R.; McDonald, K. 1981. Defect detection in lumber: state of art. For. Prod. J. 31(1):34-43.

Taylor, F.W.; Wagner, F.G.; McMillan, C.W.; Morgan, I.L.; Hopkins, F.F. 1984. Locating knots by industrial tomography - a feasibility study. For. Prod. J. 34(5):42-46.

Taylor, I.E.P.; Tepfer, M.; Callaghan, P.T.; MacKay, A.L.; Bloom, M. 1983. Use of 1H NMR to study molecular motion in cellulose, pectin and bean cell walls. J. Appl. Polym. Sci. 37:377-384.

Taylor, J.A.; Morgan, I.L.; Ellinger, H. 1980. Examination of power poles by computerized tomography. IRG Secretariat, Stockholm, Sweden, August 25, 1980. 4p.

Thornton, J.D.; Creffield, J.W.; Collett, O. 1981. On the laboratory use of X-rays in timber decay evaluation. Document IRG/WP/2144, IRG Secretariat, Stockholm, Sweden. 7p.

Tochigi, T.; Onose, K.; Satoh, H.; Sakatsume, K. 1983. A computer simulation of grain patterns on sawn surfaces. Mokuzai Gakkaishi 29(12):845-852.

Truman, R. 1953. X-ray pole inspection. Timber Technol. 61(2164):82-83.

Trussell, P.C.; Lambe, T.A.; Vitins, J. 1964. Method and apparatus for detecting internal damage in wood. Canadian Patent No.690,728 (July, 1964).

Wagner, F.G. 1985. Tomography log scanning research at the Mississippi Forest Products Laboratory and its potential benefit for lumber production. Proceedings of Internal Defect Scanning of Logs, Oslo, Norway, June 20-21, 1985. p.97-111.

Wang, P.C.; Chang, S.J. 1986. Nuclear magnetic resonance imaging of wood. Wood and Fiber Science 18(2):308-314.

Westergaard, R. 1986. Different operating philosophies guide Swedish sawmill industry. Logging and Sawmilling J., November, 1986:20-23.

## 8.0 ADDITIONAL REFERENCES
(Not referred to in text)

Bowen, D.K.; Elliott, J.C.; Stock, S.R.; Dover, S.D. 1986. X-Ray microtomography with syncrotron radiation. SPIE Vol.691, X-Ray Imaging II. p.94-98.

Chiang, B.S.; Gautam, S.R.; Hopkins, F.F.; Morgan, I.L. 1983. Spatial resolution in industrial tomography. IEEE Transactions on Nuclear Science Vol.NS-30(2):1671-1676.

Elliott, J.C.; Dover, D. 1985. X-ray microscopy using computerized axial tomography. J. of Microscopy 138(6):329-331.

Gilboy, W.B.; Foster, J.; Folkard, M. 1982. A tomographic gamma-ray scanner for industrial applications. Nuclear Methods in Physics Research 193(1982):209-214.

Gilboy, W.B. 1984. X and gamma ray tomography in NDE applications. Nuclear Methods in Physics Research 221(1984)193-200.

Habermehl, V.A.; Ridder, H-W.; Schmidt, S. 1986. A mobile computer-tomography system for examining locally fixed objects. Atomkernenergie Kerntechnik 48(2):94-99.

Hopkins, F.F.; Morgan, I.L.; Ellinger, H.D.; Klinkseik, R.V.; Meyer, G.A.; Thompson, J.N. 1981. Industrial Tomographic Applications. IEEE Transactions on Nuclear Science. Vol.NS-28(2):1717-1720.

Hopkins, F.F.; Morgan, I.L.; Ellinger, H.; Klinkseik, R.V. 1982. Tomographic image analysis. Materials Evaluation 40(11):1226-1228.

Reimers, P.; Goebbels, J.; Weise, H-P.; Wilding, K. 1984. Some aspects of industrial non-destructive evaluation by X-ray and gamma ray computed tomography. Nuclear Instruments and Methods in Physics Research 221(1984):201-206.

Roberts, R.A.; Ellington, W.A.; Vannier, M.W. 1985. A comparison of X-ray computed tomography, through transmission ultrasound, and low kV X-ray imaging for characterizing green-state ceramics. IN: Proc. 15th Non-Destructive Evaluation Symposium, San Antonio, Texas, April 23-25, 1985. 7p.

Sato, T.; Ikeda, O.; Yamakoshi, Y.; Tsubouchi, M. 1981. X-ray tomography for microstructural objects. Applied Optics 20(22):3880-3883.

Scientific Measurement Systems. 1982. Computerized Industrial Tomography. Preliminary Product Information, March 30, 1982. 83p.

Scientific Measurement Systems. 1985. Computed Industrial Tomographic Analyser, SMS Model 201 CItA. 2201 Donley Drive, Austin, Texas 78758, (512) 837-4712.

Scientific Measurement Systems. 1985. On-Stream Analysis of Seamless Tube Using Limited Angle Tomography. Proposal Exhibit C - PROPRIETARY. 44p.

ADDITIONAL REFERENCES, Contd.

Segal, E.; Notea, A.; Segal, Y. 1982. Dimensional information through industrial computerized tomography. Materials Evaluation 40(11):1268-1272.

Toshiba. 1986. Industrial CT Scanner, Series 3000/4000/5000/6000. Overseas Office, 3870 Jacombs Road, Richmond, B.C., (604) 270-8481